Deciphering fermionic matter: from holography to field theory

Meszéna, B.

Chapter 4

The Green's function of a $d = 2$ quantum critical metal at large k_F and small N_f

4.1 Introduction

The robustness of Landau's Fermi liquid theory relies on the protected gapless nature of quasiparticle excitations around the Fermi surface. Wilsonian effective field theory then guarantees that these protected excitations determine the macroscopic features of the theory in generic circumstances [2, 3]. Aside from ordering instabilities, there is a poignant exception to this general rule. These are special situations where the quasiparticle excitations interact with other protected gapless states. This is notably so near a symmetry breaking quantum critical point. The associated Goldstone modes should also contribute to the macroscopic physics. In $d \geq 3$ dimensions this interaction between Fermi surface excitations and gapless bosons is marginal/irrelevant and quantum critical metals can be addressed in perturbation theory as first discussed by Hertz and Millis [15, 5, 6, 16]. In 2+1 dimensions, however, the interaction is relevant and the theory is presumed to flow to a new interacting fixed point [51–53, 16]. This unknown fixed point has been offered as a putative explanation of exotic physics in layered electronic materials such as the Ising-nematic transition. As a consequence, the deciphering of this fixed point theory is one of the major open problems in theoretical condensed matter physics.

In this chapter we show that the fermionic and bosonic spectrum of the most elementary $d = 2$ quantum critical metal can be computed for small N_f in the limit that $k_F \to \infty$ is the largest scale in the problem (but the combination $N_f k_F$ is arbitrary). This strong forward scattering limit provides controlled insights into the properties of the postulated strongly interacting fixed point theory. All the results here refer to the

most elementary quantum critical metal. This is a set of N_f free spinless fermions at finite density interacting with a free massless (Goldstone) scalar through a simple Yukawa coupling. Its action reads (in Euclidean time)

$$S = \int \mathrm{d}x\mathrm{d}y\mathrm{d}\tau \left[\psi_j^\dagger \left(-\partial_\tau + \frac{\nabla^2}{2m} + \mu \right) \psi^j + \frac{1}{2} \left(\partial_\tau \phi \right)^2 + \frac{1}{2} \left(\nabla \phi \right)^2 + \lambda \phi \psi_j^\dagger \psi^j \right], \tag{4.1}$$

where $j = 1 \ldots N_f$ sums over the N_f flavors of fermions and $\mu = \frac{k_F^2}{2m}$. We will assume a spherical Fermi surface to start and consider excitations with momentum close to the Fermi momentum (as in [43]). In other words we often approximate the fermion action with

$$\begin{aligned} S &= \int \mathrm{d}x\mathrm{d}y\mathrm{d}\tau \left[\psi_j^\dagger \left(-\partial_\tau + \frac{\nabla^2}{2m} + \mu \right) \psi^j + \ldots \right] \\ &= \int_{-\Lambda_k}^{\Lambda_k} \frac{(k_F + k)\mathrm{d}k\mathrm{d}\theta}{(2\pi)^2} \mathrm{d}\tau \left[\psi_j^\dagger \left(-\partial_\tau - \frac{k_F}{m} \cdot k + \frac{k^2}{2m} \right) \psi^j + \ldots \right] \\ &= \int_{-\Lambda_k}^{\Lambda_k} \frac{(k_F)\mathrm{d}k\mathrm{d}\theta}{(2\pi)^2} \mathrm{d}\tau \left[\psi_j^\dagger \left(-\partial_\tau - \frac{k_F}{m} \cdot k \right) \psi^j + \ldots \right] \end{aligned} \tag{4.2}$$

with $k \equiv \left| \vec{k} \right| - k_F$ the momentum measured from the Fermi surface, and $\Lambda_k \ll k_F$ in accordance with our assumption that k_F is the largest scale. Note that this is subtly different from the so-called patch model where one splits the Fermi surface into subregions. We will still include the angle-dependence and the quadratic term at crucial points. Ignoring the angle dependence would ignore the leading correction to the boson propagator at low frequencies. This so-called Landau damping contribution becomes strong in the IR and the angle dependence can no longer be neglected (see e.g. [16]). The strong forward scattering limit $k_F \to \infty$ we consider here takes the leading Landau damping contribution into account.

The two features that allow us to compute the fermionic and bosonic spectrum at small N_f and large k_F (with $N_f k_F$ fixed) are:

1. Our earlier finding [48] that in the limit $N_f k_F \to 0$ (which we will refer to as $N_f \to 0$ for simplicity) — which self-consistently suppresses Landau damping and is closely related to the strong forward

scattering limit [49] — the exact fermion retarded Green's function of this model is given by an exponentially "dressed" free Green's function

$$G_{R,N_f\to 0}(r,t) = G_{R,\text{free}}(r,t)e^{I(r,t)} \tag{4.3}$$

with the exponent $I(r,t)$ a closed function in terms of the free boson and fermion Green's function. Due to this simple dressed expression the retarded Green's function and therefore the fermionic spectrum of this model can be determined exactly in the limit $N_f \to 0$. The retarded Green's function in momentum space reads

$$G_{R,N_f\to 0}(\omega,k) = \frac{1}{\omega - kv + \frac{\lambda^2}{4\pi\sqrt{1-v^2}}\sigma(\omega,k)}, \tag{4.4}$$

where σ is the solution of the equation

$$\frac{\lambda^2}{4\pi\sqrt{1-v^2}}(\sinh(\sigma) - \sigma\cosh(\sigma)) + v\omega - k - \cosh(\sigma)(\omega - kv + i\epsilon) = 0, \tag{4.5}$$

with k the distance from the Fermi surface, $v = k_F/m$ is the Fermi velocity, and $\epsilon \to 0^+$ is an $i\epsilon$ prescription that selects the correct root. This quenched $N_f \to 0$ limit ought to reliably capture the physics in the non-perturbative regime $\omega < \lambda^2$ but still above the Landau damping scale $\omega > \omega_{LD} \equiv \sqrt{\lambda^2 N_f k_F}$. This regime already describes interesting singular fixed point behavior: the spectrum exhibits non-Fermi liquid scaling behavior with multiple Fermi surfaces [48]. Eq. (4.4) is obtained by solving the non-linear defining equation for the fermionic Green's function directly. Formally this solution can also be obtained by summing up all diagrams without fermion loops (including the crossed-diagrams). The $N_f \to 0$ limit means that the boson propagator is not corrected by loops.

2. If one inspects the infinite series of corrections to the boson propogator diagram by diagram, one can show that for fermions with a linearized dispersion (strong forward scattering or equivalently $k_F \to \infty$) there is a cancellation among diagrams beyond one-loop [49]. In this limit the bosonic sector is therefore perturbatively determined, at small N_f (but arbitrary value of $N_f k_F$) even for finite

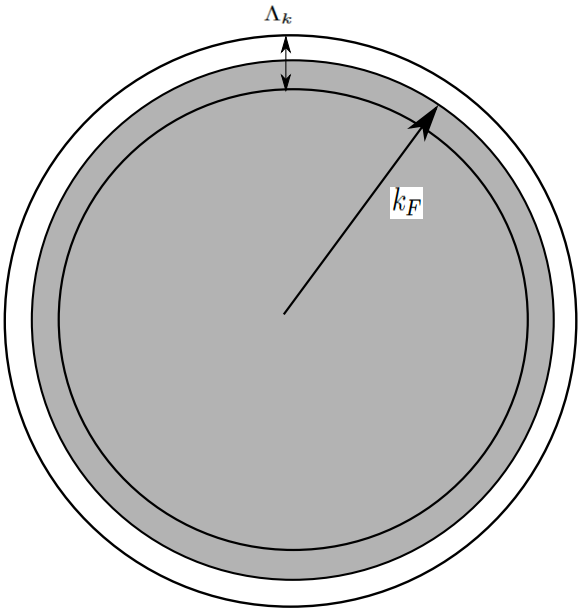

Figure 4.1. We are considering spherical surface and assume that the Fermi momentum k_F is the largest scale. The fermions have a cutoff in momentum space $k_F \gg \Lambda_k$

.

coupling. To put it another way, in the limit $k_F \to \infty$ the one-loop RPA approximation to the boson propagator becomes exact, and all bosonic higher order correlation functions vanish. The latter specifically means that the bosonic action remains quadratic and as a result one can deduce an expression of the form Eq.(4.3) with the free boson propagator replaced by the RPA summed one-loop expression.

The strong forward scattering limit has been related to an effective simplification of the fermion number Ward-identity. We review in Section 4.2 why this simplified Ward identity renders the system solvable. Using the simplified Ward-identity one can deduce a set of non-linear Schwinger-Dyson equations for the fermion and boson two-point functions alone. The vertex function drops out. As a check we recover the real space formula for the non-perturbative in λ, $N_f \to 0$ fermion propagator (in the $k_F \to \infty$ limit) we derived in our earlier paper via path integral

methods [48]. In Section 4.3 we show that the one-loop result of the boson propagator is exact in the limit $k_F \to \infty$, that higher order moments of the boson vanish, and that this also follows from the large k_F non-linear Schwinger-Dyson equations. In Section 4.4 we then show that this implies that the non-perturbative fermion propagator is given by a generalization of the quenched result where the effect of the one-loop corrected boson propagator is taken into account. With these preliminaries in hand we use the bulk of Section 4.4 to solve the non-linear large k_F equation for the fermion spectral function for small N_f —- analytically in real space and numerically in momentum space. In Section 4.5 we collect our results for the 2+1 dimensional quantum critical metal. We conclude with an outlook in Section 4.6.

4.2 A closed system of Schwinger-Dyson equations and large k_F Ward identities for the elementary quantum critical metal

The Schwinger-Dyson equations of a field theory are in general an infinite set of coupled integral equations that together determine the correlations functions exactly. Here we review that using the Ward identity associated with the $U(1)$ symmetry $\psi \to \psi \exp(i\alpha)$ the integral equations describing the relation between the fermionic Green's function G and the bosonic Green's function G_B form a closed system in the limit $k_F \to \infty$.

The Schwinger-Dyson equation which describes the fermionic propagator reads

$$G(K) = G_0(K) + \lambda G_0(K) G(K) \int \mathrm{d}Q \, G_B(Q) G(K-Q) \Gamma(K, K-Q), \tag{4.6}$$

where Q and K are shorthand notation for the collection of momentum and euclidean frequency variables $Q = (iq_0, \vec{q})$, $\mathrm{d}Q = \frac{\mathrm{d}q_0 \mathrm{d}^2\vec{q}}{(2\pi)^3}$; $\Gamma(K, K-Q)$ is the 1PI 3-point vertex and

$$G_0(K) = \frac{1}{ik_0 - \frac{1}{2m}\left(\vec{k}^2 - k_F^2\right)} \tag{4.7}$$

is the free fermion propagator. For completeness we give its derivation in Appendix 4.A.

The analogous boson Schwinger-Dyson equation[1]

$$G_B(Q) = G_{B,0}(Q) - \lambda N_f G_{B,0}(Q) G_B(Q) \int \mathrm{d}K\, G(K) G(K-Q) \Gamma(K, K-Q) \tag{4.8}$$

can be recast in terms of the boson polarization (self-energy) $\Pi \equiv G_B^{-1} - G_{B,0}^{-1}$.

$$\Pi\left(Q\right) = \lambda N_f \int \mathrm{d}K\, G\left(K+Q/2\right) G(K-Q/2) \Gamma(K+Q/2, K-Q/2), \tag{4.9}$$

with

$$G_{B,0} = \frac{1}{q_0^2 + \vec{q}^2}. \tag{4.10}$$

the free boson propagator. This polarization term captures the non-trivial physics of Landau damping.

Usually the system of Schwinger-Dyson equations does not close because the equation for the three-point vertex Γ contains higher point vertices $\Gamma^{(n)}$. For finite k_F the same is true in the model of the elementary quantum critical metal. However, the fermion number symmetry implies a Ward identity between G and Γ. At finite k_F this identity also includes other components Γ^i of the fermion number current. What has been noted for this and similar theories is that for large k_F the current components are proportional to Γ (see e.g. [38, 49, 56]) and the Ward identity collapses to

$$\Gamma\left(P, Q\right) = \lambda \frac{G^{-1}\left(P\right) - G^{-1}\left(Q\right)}{i(p_0 - q_0) - \left(\frac{\vec{p}^2}{2m} - \frac{\vec{q}^2}{2m}\right)} + \ldots. \tag{4.11}$$

We have modified the result obtained there slightly by terms that also vanish as $k_F \to \infty$ such that at lowest order $\Gamma = \lambda + \ldots$ as it should.

Using the large k_F form of the Ward identity (4.11), where we drop the $\ldots$ terms, the Schwinger-Dyson equations (4.6) and (4.9) become a

[1] The extra minus sign is from the fermion loop.

closed set of equations for G_B and G

$$G(K) = G_0(K) + \lambda^2 G_0(K) \int \mathrm{d}Q\, G_B(Q) \frac{G(K-Q) - G(K)}{iq_0 + v\frac{\vec{q}^2}{2k_F} - v|\vec{q}|\cos\theta - v\frac{k}{k_F}|\vec{q}|\cos\theta}, \tag{4.12}$$

$$\Pi(Q) = \lambda^2 N_f \int \mathrm{d}K \frac{G(K-Q/2) - G(K+Q/2)}{iq_0 - v|\vec{q}|\cos\theta - v\frac{k}{k_F}|\vec{q}|\cos\theta}, \tag{4.13}$$

which should become exact in the limit $k_F \to 0$. Here θ is the angle between $\vec{k}$ (measured from the origin) and $\vec{q}$.

Note that the large k_F limit of the Ward identity is crucial to derive this closed set. Therefore, we will drop the subleading terms from the denominators such as k/k_F and $\vec{q}^2/k_F$. The solutions to this closed set of integral equations determine the two-point functions at large k_F and hence the spectrum of the elementary quantum critical metal. We now proceed to study and solve this closed set of equations in the limit $k_F \to \infty$.

4.2.1 The $k_F \to \infty$ limit of the Schwinger-Dyson equations and the fermion two-point function: formal connection with the quenched result

Let us study the consequences of the large k_F limit of the fermion SD-equation (4.12). In this approximation it can be written as

$$\frac{G(k_0,k)}{G_0(k_0,k)} = 1 + \lambda^2 \int \frac{\mathrm{d}q_0 \mathrm{d}q_x}{(2\pi)^2} \mathcal{K}(q_0,q_x) \left[G(k_0-q_0,k-q_x) - G(k_0,k)\right], \tag{4.14}$$

with the kernel

$$\mathcal{K}(q_0,q_x) = \int \frac{\mathrm{d}q_y}{2\pi} \frac{G_B(Q)}{iq_0 - vq_x} \tag{4.15}$$

where $q_x = |\vec{q}|\cos\theta$, $q_y = |\vec{q}|\sin\theta$, i.e. we have aligned the $\vec{q}$-integral with the external momentum $\vec{k}$. In the arguments of the full Green's function $G(k_0,k)$ in Eq. (4.14) we have used the fact that because of spherical symmetry $G(k_0,k)$ can only depend on the distance to the Fermi surface $k = |\vec{k}| - k_F$. In addition, for the spatial argument of $G(K-Q)$ we

have used that $|\vec{k}-\vec{q}|-k_F \approx k-q_x+\mathcal{O}\left(\vec{q}^2/k_F\right)$. The same argument applied to the free fermion propagator $G_0=\frac{1}{iq_0-vq_x}+\ldots$ shows that the denominator in the definition of the kernel in Eq.(4.15) becomes equivalent to G_0. In other words

$$\mathcal{K}(q_0,q_x)=G_0(q_0,q_x)\int\frac{\mathrm{d}q_y}{2\pi}G_B(Q) \tag{4.16}$$

Note that using the notation $G_0(q_0,q_x)$ in the definition of the kernel is somewhat formal. Of course as we mentioned the fermion Green's function is spherically symmetric. To analyze Eq.(4.14) we assume that parity remains unbroken and $G_B\left(Q\right)=G_B\left(-Q\right)$ holds non-perturbatively. Then the term $\int\frac{\mathrm{d}q_0\mathrm{d}q_x}{(2\pi)^2}\mathcal{K}\left(q_0,q_x\right)G\left(k_0,k\right)$ vanishes. We can then solve this integral equation by converting to a differential equation. For this we note that the remaining term on the right-hand side of Eq.(4.14) is a convolution of $\mathcal{K}$ and G, therefore it is advantegeous to write the equation in position space. In position space the term $G_0^{-1}\left(k_0,k\right)=ik_0-vk$ on the left-hand side turns into a differential operator. The position space version of equation (4.14) is

$$\left(\partial_\tau-iv\partial_r\right)G\left(\tau,r\right)=\delta^2(\tau,r)+\lambda^2\mathcal{K}\left(\tau,r\right)G\left(\tau,r\right). \tag{4.17}$$

where we have used the Fourier transform convention

$$G(\tau,r)=\int\frac{\mathrm{d}k_0\mathrm{d}k}{(2\pi)^2}G\left(k_0,k\right)\exp\left(-ik_0\tau+ik\cdot r\right), \tag{4.18}$$

The solution to Eq. (4.17) can be found by using the ansatz $G\left(\tau,r\right)=G_0\left(\tau,r\right)\exp\left(I(\tau,r)\right)$ with the exponent $I(\tau,r)$ satisfying

$$\left(\partial_\tau-iv\partial_r\right)I(\tau,r)=\lambda^2\mathcal{K}\left(\tau,r\right), \tag{4.19}$$

with the boundary condition $I(0,0)=0$.

Since $G_0(\tau,r)$ is the Green's function of the differential operator in Eq. (4.19), the solution for $I(\tau,r)$ is formally given by

$$I(\tau,r)=\lambda^2\int\mathrm{d}r'\mathrm{d}\tau'\left[G_0\left(\tau-\tau',r-r'\right)-G_0\left(-\tau',-r'\right)\right]\mathcal{K}\left(\tau',r'\right). \tag{4.20}$$

By transforming $G_0(\tau,r)$ and $\mathcal{K}(\tau,r)$ back to momentum space we arrive at the expression for the exponent

$$I\left(\tau,r\right)=\lambda^2\int\frac{\mathrm{d}k_0\mathrm{d}k\mathrm{d}k_y}{(2\pi)^3}G_0^2\left(k_0,k\right)G_B\left(k_0,k,k_y\right)\left[\cos\left(ik_0\tau-ikr\right)-1\right]. \tag{4.21}$$

We have used the fact that $G_0^2(K)\,G_B(K)$ is symmetric in K.

We now see the drastic simplification that occurs in the limit $k_F \to \infty$. The solution to the exact fermion Green's function in this limit only depends on the exact boson Green's function $G_B(K)$. Once the latter is known, the fermion Green's function G follows and it in turn determines the exact 1PI three-point vertex Γ.

We noted this exponential form of the fully non-perturbative solution already in the previous chapter [48] that discussed the elementary quantum critical metal in the quenched limit $N_f \to 0$ (see also [36]). In that limit $N_f \to 0$, the polarization Π vanishes and the exact boson propagator $G_B(K)$ in Eq. (4.21) can be replaced by the free one $G_{B,0}(K)$. The explicit expression for the exponent $I(\tau, r)$ and thus the non-perturbative fermion two-point function is then formally known, up to the remaining momentum integrals. These have been evaluated for the quenched $N_f \to 0$ case in [48] with the interesting result that even in the absence of corrections to the boson propagator — the absence of Landau damping — the system already resembles that of a non-trivial fixed point. We now proceed by considering the finite N_f polarization corrections in $I(\tau, r)$. Of course we do so in the same limit $k_F \to \infty$.

4.3 The $k_F \to \infty$ limit of the Schwinger-Dyson equations and the exact boson two-point function

We now turn to the study of the boson two-point function. Diagrammatic studies in perturbation theory have shown that the theory simplifies in the limit $k_F \to \infty$ [49]. In particular, as we shall derive below in section 4.3.3, all n-point scalar correlation functions with $n > 2$ vanish. As a corollary the 1PI boson 2-point function is only corrected at one-loop. This suggests that the solution to the Schwinger-Dyson equations should be more readily obtainable in this limit as well.

We show in this section that the large k_F approximation has such an important simplifying consequence for the bosonic equation. The important physics we refer to is the physics of Landau damping — fermionic corrections to the boson propagator — discussed in the introduction. In this elememtary quantum critical metal, where the boson has no self-interactions, this physics is contained in the polarization $\Pi = G_B^{-1} - G_{B,0}^{-1}$.

Generically the calculation of the polarization Π corresponds to summing up infinitely many diagrams as the Schwinger-Dyson equation (4.13) contains the exact fermion propagator G. However, in the limit $k_F \to \infty$ only the one-loop contribution Π_1 survives (for small N_f at least). The realization that in this strong forward scattering limit many diagrams vanish and only the boson two-point function gets corrected is not new; it has been noted earlier in e.g. [49]. We independently rederive it here. First, however, we will give the one-loop result. Based on that one can give a proof why all higher order corrections vanish.

4.3.1 Polarization/Landau damping contribution at one-loop

The $k_F \to \infty$ one-loop contribution to the polarization that captures the leading order physics of Landau damping is obtained by substituting the $k_F \to \infty$ limit of the free fermion propagator $G_0(k_0, k) = \frac{1}{ik_0 - vk} + \ldots$ into the Schwinger-Dyson equation (4.13) and also taking $k_F \to \infty$ in the remaining terms. The result is

$$\Pi_1(Q) = \lambda^2 N_f k_F \int \frac{\mathrm{d}k_0 \mathrm{d}k d\theta}{(2\pi)^2} \frac{1}{(ik_0 - vk)\left(i\left(k_0 + q_0\right) - v\left(k + |\vec{q}|\cos\theta\right)\right)}. \tag{4.22}$$

The result of these integrals is finite but depends on the order of integration. The difference is a constant C

$$\Pi_1(Q) = \frac{\lambda^2 k_F N_f}{v}\left(\frac{|q_0|}{\sqrt{q_0^2 + v^2\vec{q}^2}} + C\right). \tag{4.23}$$

As pointed out for instance for the 3+1 dimensional quantum critical metal in [29], the way to think about this ordering ambiguity is that one should strictly speaking first regularize the theory and introduce a one-loop counterterm. This counterterm has a finite ambiguity that needs to be fixed by a renormalization condition. Even though the loop momentum integral happens to be finite in this case, the finite counterterm ambiguity remains. The correct renormalization condition is the choice $C = 0$. This choice corresponds to the case when the boson is tuned to criticality since a non-zero C would mean the presence of an effective mass generated by quantum effects.

A more physical way to think of the ordering ambiguity is as the relation between the frequency (Λ_0) and momentum (Λ_k) cutoff. We will assume that $\Lambda_k \gg \Lambda_0$ — which means that we evaluate the k integral first and then the frequency k_0 integral. In this case $C = 0$ directly follows.

4.3.2 The solution to the $k_F \to \infty$ Schwinger-Dyson equation: Robustness of the one-loop result

We will now give a heuristic derivation that the one-loop result is in fact the exact answer in the limit $k_F \to \infty$. The full polarization Schwinger-Dyson equation (4.13) in the limit $k_F \to \infty$ can be written as

$$\Pi(q_0, q) = \lambda^2 k_F N_f \int \frac{\mathrm{d}k_0 \mathrm{d}k \mathrm{d}\theta}{(2\pi)^2} \frac{G(k_0 - q_0/2, k) - G(k_0 + q_0/2, k)}{iq_0 - vq\cos\theta} = \frac{-2\pi i \operatorname{sgn} q_0}{\sqrt{q_0^2 + v^2 q^2}} \lambda^2 k_F N_f \int \frac{\mathrm{d}k_0 \mathrm{d}k}{(2\pi)^2} \left[G(k_0 - q_0/2, k) - G(k_0 + q_0/2, k)\right], \tag{4.24}$$

where $q = |\vec{q}|$. Following our discussion above that regularizing and renormalizing with a counterterm is the same as the prescription to perform the momentum integral first, we may shift the momentum integral so that in the difference both Green's functions have the same momentum in their argument. We are not allowed to do this subsequently again for the frequency integral, since $\int dk_0 dk G(k_0, k) = \infty$. One needs to evaluate the frequency integral with an explicit cutoff Λ_0 which can be removed in the end.

The integrand of the frequency integration:
$\int \mathrm{d}k \left[G(k_0 - q_0/2, k) - G(k_0 + q_0/2, k)\right]$, clearly vanishes as $q_0 \to 0$. Expanding around q_0 (in units of the cut-off Λ_0) one has

$$\begin{aligned} \int_{-\Lambda_0}^{\Lambda_0} \mathrm{d}k_0 \int \mathrm{d}k \left[G(k_0 - q_0/2, k) - G(k_0 + q_0/2, k)\right] \\ = -\frac{q_0}{2} \int \mathrm{d}k_0 \frac{d}{dk_0} \left[G(k_0, k) + G(k_0, k)\right] + \mathcal{O}\left(\frac{q_0^2}{\Lambda_0^2}\right) \\ = -q_0 \int \mathrm{d}k \left[G(\Lambda_0, k) - G(-\Lambda_0, k)\right] + \ldots \end{aligned} \tag{4.25}$$

Because the coupling constant of the theory is relevant we can replace the exact, interacting fermion propagator evaluated at $k_0 = \pm\Lambda_0$ with the

free one $G(\Lambda_0, k) \approx G_0(\Lambda_0, k)$. Doing so we arrive to the result of (4.23). This heuristically shows the robustness of the one-loop result. The one caveat is the value of Π for large external momenta q_0 near the cut-off. We now show by an different method that the one-loop result is in fact exact to all orders.

4.3.3 Multiloop cancellation

The robustness of the one-loop result in case of linear fermionic dispersion was recognized before under the name of multiloop cancellation [49]. The technical result is that for a theory with a simple Yukawa coupling and linear dispersion around a Fermi surface, a symmetrized fermion loop with more than two fermion lines vanishes. In our context the linear dispersion is a consequence of the large k_F limit. In other words all higher loop contributions to the polarization Π should be subleading in $1/k_F$. This was explicitly demonstrated at two loops in [55].

Note that there still can be diagrams which contain a subpiece which is subleading in the above sense but the rest of the diagram renders the whole finite. However, in this case multiple fermions running around in the diagram. Therefore, it scales with positive power of N_f (without k_F multiplier) and it is not included in the first order small N_f result.

We will give here a short derivation of this multiloop cancellation in the limit $k_F \to \infty$. As before (below Eq. (4.15)) we may assume in this limit that the momentum transfer at any fermion interaction is always much smaller than the size of the initial ($\vec{k}$) and final momenta ($\vec{k}'$) which are of the order of the Fermi momentum, i.e. $|\vec{k}' - \vec{k}| \ll k_F$ with $|\vec{k}|, |\vec{k}'| \sim k_F$. The free fermion Green's function then reflects a linear dispersion

$$G_0(\omega, k) = \frac{1}{i\omega - vk} \tag{4.26}$$

We now Fourier transform back to real space, as multiloop cancellation is most easily shown in this basis. The real space transform of the "linear" free fermion propagator above is

$$G_0(\tau, r) = -\frac{i}{2\pi} \frac{\mathrm{sgn}(v)}{r + iv\tau}, \tag{4.27}$$

where as before r is the conjugate variable to $k = |\vec{k}| - k_F$. The essential step in the proof is that real space Green's function manifestly obeys the

identity [48]

$$G_0(z_1)\,G_0(z_2) = G_0(z_1+z_2)\,(G_0(z_1)+G_0(z_2)) \tag{4.28}$$

with $z \equiv r + iv\tau$. Consider then (the subpart of any correlation function/Feynman diagram containing) a fermion loop with $n \geq 2$ vertices along the loop connected to indistinguishable scalars (i.e. no derivative interactions and all interactions are symmetrized). The corresponding algebraic expression in a real space basis will then contain the expression

$$F(z_1,...,z_n) = \sum_{(i_1,..,i_n)\in S_n} G_0(z_{i_1}-z_{i_2})\,G_0(z_{i_2}-z_{i_3})\,...G_0(z_{i_{n-1}}-z_{i_n}) \cdot G_0(z_{i_n}-z_{i_1})\,, \tag{4.29}$$

where S_n is the set of permutations of the numbers 1 through n. Using the "linear dispersion" identity Eq. (4.28) and the shorthand notation $G_0(z_{i_1}-z_{i_2}) = G_{12}$ we obtain

$$F(z_1,...,z_n) = \sum_{(i_1,..,i_n)\in S_n} G_{12}G_{23}...G_{n-1,1}\,(G_{n-1,n}+G_{n,1})\,. \tag{4.30}$$

Next we cyclically permute the indices from 1 to $n-1$: $1\to 2$, $2\to 3$, ..., $n-1\to 1$ in the sum

$$\sum_{(i_1,..,i_n)\in S_n} G_{12}G_{23}...G_{n-1,1}G_{n-1,n} = \sum_{(i_1,..,i_n)\in S_n} G_{23}G_{34}...G_{12}G_{1,n}. \tag{4.31}$$

This gives us

$$F(z_1,...,z_n) = \sum_{(i_1,..,i_n)\in S_n} G_{12}G_{23}...G_{n-1,1}\,(G_{1,n}+G_{n,1})\,. \tag{4.32}$$

Then since $G_{i,j}$ corresponds to a (spinless) fermionic Green's function, it is antisymmetric $G_{i,j} = -G_{j,i}$, and we can conclude that F vanishes for $n \geq 3$. For $n = 2$ it is not possible to use the identity Eq. (4.28) since we would need to evaluate $G(0)$ which is infinite.

4.4 The fermion two-point function in the limit $k_F \to \infty$ at small N_f

4.4.1 The exact fermionic two-point function in real space: an analytical form

We have thus established that the exact boson two-point function including Landau-damping is completely given by the Dyson-summed one-loop expression in the limit $k_F \to \infty$, and that this one-loop polarization arguably faithfully captures the low-energy physics. We can now use this exact boson two-point function to determine the exact fermion two-function from the formal solution to the large k_F Ward-Schwinger-Dyson equations (in real space)

$$G(\tau, r) = G_0(\tau, r) e^{I(\tau, r)} \tag{4.33}$$

with (see Eq. (4.21))

$$I(\tau, r) = \lambda^2 \int \frac{\mathrm{d}\omega \mathrm{d}k_x \mathrm{d}k_y}{(2\pi)^3} G_0^2(\omega, k_x) G_B(\omega, k_x, k_y) \left[\cos(\omega\tau - k_x r) - 1\right]. \tag{4.34}$$

Substituting in the exact boson two-point function $G_B = 1/(G_{B,0}^{-1} + \Pi)$, we thus need to calculate the integral

$$I(\tau, r) = \lambda^2 \int \frac{\mathrm{d}\omega \mathrm{d}k_x \mathrm{d}k_y}{(2\pi)^3} \frac{\cos(\tau\omega - r k_x) - 1}{(i\omega - k_x v)^2 \left(\omega^2 + k_x^2 + k_y^2 + \frac{4\pi^2 \lambda^2 N_f k_F |\omega|}{v\sqrt{v^2(k_x^2 + k_y^2) + \omega^2}}\right)}. \tag{4.35}$$

In this expression and the following sections we have rescaled $N_f k_F$ to $(2\pi)^2 N_f k_F$. That is where the factor $4\pi^2$ comes from.

Intermezzo — The large-$N_f k_F$ limit: a comparison to previous approaches

An often used approximation in the literature is to take the IR limit of the boson propagator, see e.g [38, 16]. In this limit the polarisation term will dominate over the kinetic terms, but since the rest of the integrand in (4.35) has no k_y dependence, it is necessary to keep the k_y term in the boson propagator. This simplification is expected to be better with

increasing $N_f k_F$. We therefore refer to the simplified boson two-point function as the large $N_f k_F$ propagator

$$G_{B,N_f k_F\to\infty}(\omega,k_x,k_y)=\frac{1}{k_y^2+\frac{4\pi^2\lambda^2 N_f k_F|\omega|}{v^2|k_y|}}. \tag{4.36}$$

This Landau-damped propagator has been used extensively, for instance [16, 38]. In [38] this propagator was used for the type of non-perturbative calculation we are proposing here. We discuss this here, as we will now show that using this simplified propagator for our method has a problematic feature. In short, this propagator only captures the leading large $N_f k_F$ contribution but the non-perturbative exponential form of the exact Green's function sums up powers of the propagator which then are subleading in $N_f k_F$. We will use therefore the full bosonic propagator which will also enable us to compare our results with our previous quenched calculation. Let us, however, first show explicitly the problems that arise with the simplified propagator.

In the large $N_f k_F$ limit the integral $I(\tau,r)$ to be evaluated simplifies to

$$I_{N_f k_F\to\infty}=\lambda^2\int\frac{\mathrm{d}\omega\mathrm{d}k_x\mathrm{d}k_y}{(2\pi)^3}\frac{\cos(\tau\omega-xk_x)-1}{(i\omega-k_x v)^2\left(k_y^2+\frac{4\pi^2\lambda^2 N_f k_F|\omega|}{v^2|k_y|}\right)}. \tag{4.37}$$

After evaluating the k_x integral:

$$I_{N_f k_F\to\infty}=-\lambda^2\int\frac{\mathrm{d}\omega\mathrm{d}k_y}{(2\pi)^3}\frac{\pi k_y^2|r|e^{-|\omega|\left(\frac{|r|}{v}+i\,\mathrm{sgn}(r)\tau\right)}}{4\pi^2\lambda^2 N_f k_F\,|\omega k_y|+k_y^4 v^2}. \tag{4.38}$$

The k_y integral can be performed next to yield

$$I_{N_f k_F\to\infty}=-\lambda^2\int\mathrm{d}\omega\frac{(2\pi)^{-5/3}\,|r|\,e^{-|\omega|\left(\frac{|r|}{v}+i\,\mathrm{sgn}(r)\tau\right)}}{3\sqrt{3}v^{4/3}(\lambda^2 N_f k_F\,|\omega|)^{1/3}}. \tag{4.39}$$

The primitive function to this ω integral is the upper incomplete gamma function, with argument $2/3$. Evaluating this incomplete gamma function in the appropriate limits and substituting the final expression for $\underset{N_f k_F\to\infty}{I}(\tau,r)$ into the expression for the fermion two-point function gives us:

$$\underset{Nfk_F\to\infty}{G_f}(\tau,r)=\frac{1}{2\pi(ir-v\tau)}\exp\left(-\frac{|r|}{l_0^{1/3}\left(|r|+iv\,\mathrm{sgn}(r)\tau\right)^{2/3}}\right) \tag{4.40}$$

where the length scale l_0 is given by

$$l_0^{1/3} = \frac{3\sqrt{3}(2\pi)^{5/3}v^{2/3}(N_f k_F)^{1/3}}{2\Gamma\left(\frac{2}{3}\right)\lambda^{4/3}}. \tag{4.41}$$

This result has been found earlier in [37] (see also [49]). It is much more instructive to study, however, the momentum space version of the propagator. The Fourier transform of the real space Green's function

$$\underset{N_f k_F\to\infty}{G_f}(\omega,k) = \int \mathrm{d}\tau\mathrm{d}r \frac{\mathrm{e}^{i(\omega\tau-kr)}}{2\pi(ir-v\tau)} \exp\left(-\frac{|r|}{l_0^{1/3}\left(|r|+iv\,\mathrm{sgn}(r)\tau\right)^{2/3}}\right) \tag{4.42}$$

is tricky, but remarkably can be done exactly. We do so in appendix 4.B. The result is

$$\begin{aligned}\underset{N_f k_F\to\infty}{G_f}(\omega,k) =& \frac{1}{i\omega-kv}\cos\left(\frac{\omega}{v l_0^{1/2}(\omega/v+ik)^{3/2}}\right)\\ &+\frac{6\sqrt{3}i\Gamma\left(\frac{1}{3}\right)\omega^{2/3}}{8\pi l_0^{1/3}v^{5/3}(\omega/v+ik)^2}\,{}_1F_2\left(1;\frac{5}{6},\frac{4}{3};-\frac{\omega^2}{4l_0v^2(\omega/v+ik)^3}\right)+\\ &+\frac{3\sqrt{3}i\Gamma\left(-\frac{1}{3}\right)\omega^{4/3}}{8\pi l_0^{2/3}v^{7/3}(\omega/v+ik)^3}\,{}_1F_2\left(1;\frac{7}{6},\frac{5}{3};-\frac{\omega^2}{4l_0v^2(\omega/v+ik)^3}\right).\end{aligned} \tag{4.43}$$

This expression has been compared with numerics to verify its correctness; see Fig. 4.2.

Recall that Eq. (4.43) is the Green's function in Euclidean signature. Continuing to the imaginary line, $\omega = -i\omega_R$, this becomes the proper retarded Greens function, $G_R(\omega_R,k)$, and from this we can obtain the spectral function $A(\omega_R,k) = -2\mathrm{Im}\ G_R(\omega_R,k)$. As it encodes the excitation spectrum, the spectral function ought to be a positive function that moreover equals 2π when integrated over all energies ω_R, for any momentum k. This large $N_f k_F$ spectral function contains an oscillating singularity at $\omega_R = vk$. We are free to move the contour into complex ω_R-plane by deforming $\omega_R \to \omega_R + i\Omega$ where Ω is positive but otherwise arbitrary. Upon doing this it is easy to numerically verify that indeed the integral over ω_R gives 2π. However, if we look at the behaviour close to the essential singularity the function oscillates rapidly and does not stay positive as one approaches the singularity; see Fig. 4.3. This reflects that

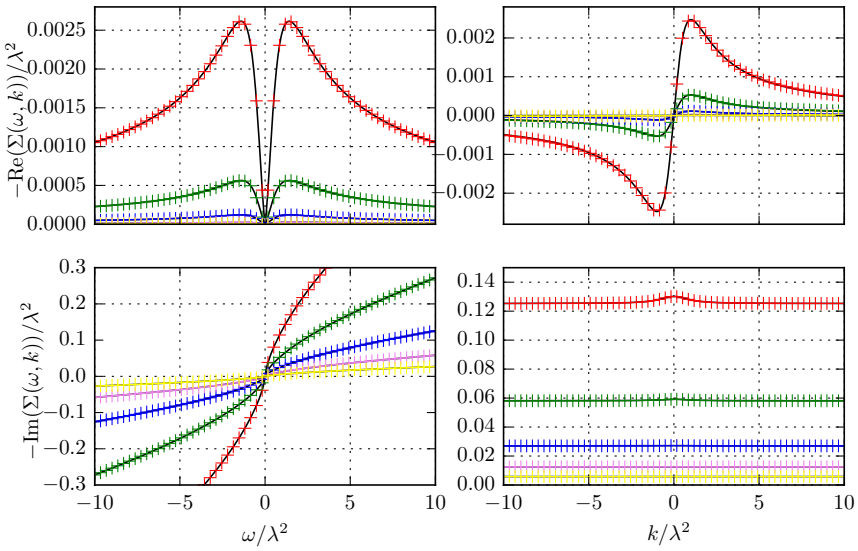

Figure 4.2. Real and imaginary parts of the self energy obtained using the large-$N_f k_F$ Landau-damped propagator. This plot shows the agreement between the numerics and the analytical solution, verifying that both solutions are correct. Notice the difference in magnitude between the real and imaginary part. The agreement of the real parts shows that the numerical procedure has a very small relative error. All plots are for the $k, \omega = \lambda^2$ slice with $v = 1$.

the large $N_f k_F$ approximation done in this way is not consistent. Even though the approximation for the exponent $I(\tau, r) \equiv \frac{\tilde{I}(\tau,r)}{(N_f k_F)^{1/3}}$ is valid to leading order in $1/(N_f k_F)$, this is not systematic after exponentiation to obtain the fermion two-point function

$$\underset{N_f k_F \to \infty}{G_f}(\tau, r) = \frac{1}{2\pi(ir - v\tau)} \exp\left(\frac{\tilde{I}(\tau, r)}{(N_f k_F)^{1/3}} + \mathcal{O}\left(\frac{1}{(N_f k_F)^{2/3}} \right) \right). \tag{4.44}$$

Reexpanding the exponent one immediately sees that keeping only the leading term in $I(\tau, r)$ mixes at higher order with the subleading terms at lower order in $1/N_f k_F$

$$\underset{N_f k_F \to \infty}{G_f}(\tau, x) = \frac{1}{2\pi(ir - v\tau)} \left(1 + \frac{\tilde{I}(\tau, r)}{(N_f k_F)^{1/3}} + \mathcal{O}\left(\frac{1}{(N_f k_F)^{2/3}} \right) + \frac{1}{2}\left(\frac{\tilde{I}(\tau, r)}{(N_f k_F)^{1/3}} + \dots \right)^2 \right). \tag{4.45}$$

Nevertheless, we will see that in the IR $\underset{N_f k_F \to \infty}{G_f}$ (with a small modification) capture the physics very well.

Exact large k_F fermion two-point function; $v = 1$

To get the general $N_f k_F$ answer we return to the full integral Eq.(4.35) needed to determine the real space fermion two-point function. Solving this in general is difficult, and to simplify mildly we consider the special case $v = 1$. In our previous studies of the quenched $N_f k_F = 0$ limit we saw that this case is actually not very special. In fact, nothing abruptly happens as $v \to 1$, except that the quenched $N_f k_F = 0$ solution can be written in closed form for this value of $v = 1$. Nor for the case of large $N_f k_F$ is the choice $v = 1$ in any way special. As can be seen above in Eq. (4.40) for large $N_f k_F$ all v are equivalent up to a rescaling of τ versus r and a rescaling of the single length scale l_0. We may therefore expect that for a finite N_f, the physics of $0 < v < 1$ is qualitatively the same as the (not-so-) special case $v = 1$.

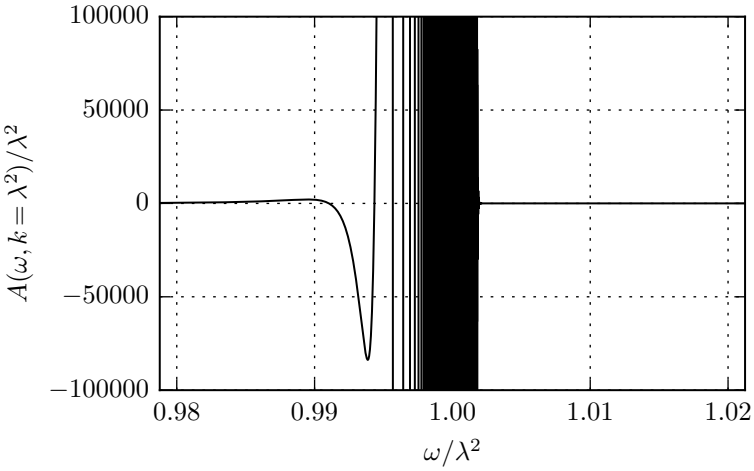

Figure 4.3. Exact fermion spectral function based on the large-$N_f k_F$ approximation for the exact boson propagator. Notice that the function is not positive everywhere. Here $k = \lambda^2$, $v = 1$ and $N_f k_F = \lambda^2$.

After setting $v = 1$ and changing to spherical coordinates we have

$$I = \int \mathrm{d}\tilde{r}\mathrm{d}\phi\mathrm{d}\theta \mathrm{e}^{2i\phi} \frac{\cos\Big(\tilde{r}\sin(\theta)(\tau\sin(\phi) - r\cos(\phi))\Big) - 1}{8\pi^3 \sin(\theta)^2 \Big(N_f k_F \pi^2 |\sin(\phi)| + \lambda^{-2}\tilde{r}^2/\sin(\theta)\Big)} \,. \tag{4.46}$$

Performing the $\tilde{r}$ integral gives us

$$I = \lambda \int \mathrm{d}\phi\mathrm{d}\theta \mathrm{e}^{2i\phi} \frac{\mathrm{e}^{-2\pi\lambda|\tau\sin(\phi) - r\cos(\phi)|\sqrt{N_f k_F |\sin(\phi)| \sin(\theta)^3}} - 1}{32\pi^3 \sqrt{N_f k_F |\sin(\phi)| \sin(\theta)^3}} \,. \tag{4.47}$$

Note that if the signs of both τ and r are flipped, then this is invariant. Changing the sign of only τ, and simultaneously making the change of variable $\phi \to -\phi$, then the (real) fraction is invariant but the exponent in the prefactor changes sign. Thus, I goes to I^* as the sign of either τ or r is changed. Without loss of generality, we can assume that both of them are positive from now on. We further see that the integrand is invariant under $\phi \to \phi + \pi$, so we may limit the range of ϕ to $(0, \pi)$ by doubling the value of integrand. Similarly we limit θ to $(0, \pi/2)$ and multiply by

another factor of 2. We then make the changes of variables:

$$\begin{aligned}\phi &= \tan^{-1}(s) + \pi/2 \\ \theta &= \sin^{-1}(u^{2/3})\end{aligned} \tag{4.48}$$

with $s \in \mathbb{R}$ and u is integrated over the range $(0, 1)$. For convenience we introduce the function

$$z(s) = \frac{\pi}{2}\lambda\sqrt{N_f k_F}|sr + \tau|(1+s^2)^{-3/4} \tag{4.49}$$

Now the two remaining integrals can be written as

$$I = \lambda \int \mathrm{d}s\mathrm{d}u \frac{(\mathrm{e}^{-4uz(s)} - 1)(s-i)}{12\pi^3(s+i)(1+s^2)^{3/4}u^{4/3}\sqrt{N_f k_F(1-u^{4/3})}} \tag{4.50}$$

After expanding the exponential we can perform the u integral term by term. We are left with

$$I = \lambda \int \mathrm{d}s \sum_{n=1}^{\infty} \frac{4^{n-2}(1+s^2)^{1/4}(-z(s))^n}{\pi^{5/2} n! \sqrt{N_f k_F}(i+s)^2} \frac{\Gamma\left(\frac{3n-1}{4}\right)}{\Gamma\left(\frac{3n+1}{4}\right)} \tag{4.51}$$

This can be resummed into a sum of generalized hypergeometric functions, but this is not useful at this stage. Instead we once again integrate term by term. Collecting the prefactors and introducing the constant $a = \tau/r$, the n-th term can be written as

$$I = \sum_{n=1}^{\infty} c_n \int \mathrm{d}s\, (s-i)^2 |s+a|^n (1+s^2)^{-(7+3n)/4} \tag{4.52}$$

This can be written as

$$I = \sum_{n=1}^{\infty} c_n \int \mathrm{d}s\mathrm{d}w\, (s-i)^2 |s+a|^n \frac{\mathrm{e}^{-w(s^2+1)} w^{3(1+n)/4}}{(3(1+n)/4)!} \tag{4.53}$$

where w is integrated on $(0, \infty)$. After splitting the integral at $s = -a$ to get rid of the absolute value we can calculate the s integrals in terms of confluent hypergeometric functions ${}_1F_1(a, b; z)$. Adding the two halves

$s < -a$ and $s > -a$ of the integral we have

$$I = \sum_{n=1}^{\infty} c_n \int \mathrm{d}w \frac{\Gamma\left(\frac{1+n}{2}\right)\mathrm{e}^{-(1+a^2)w}}{2(3(1+n)/4)!} \left(2w(i+a)^2 \ {}_1F_1\left(\frac{2+n}{2}, \frac{1}{2}; a^2 w\right) \right.$$
$$\left. + (2+n) \ {}_1F_1\left(\frac{4+n}{2}, \frac{1}{2}; a^2 w\right) - 4aw(2+n)(i+a) \ {}_1F_1\left(\frac{4+n}{2}, \frac{3}{2}; a^2 w\right) \right). \tag{4.54}$$

It may look like we have just exchanged the s-integral for the w-integral, but by writing the hypergeometric functions in series form,

$$I = \sum_{n=1}^{\infty} c_n \int \mathrm{d}w \sum_{m=0}^{\infty} \frac{2^{2m-1} a^{2m} \mathrm{e}^{-(1+a^2)w} w^{\frac{n-3}{4}+m} \Gamma\left(\frac{1+n}{2}+m\right)}{\Gamma\left(\frac{7+3n}{4}\right)\Gamma\left(2+2m\right)} \cdot$$
$$\cdot \left(n(1+2m-4a(i+a)w) + (1+2m)(1+2m-2(1+a^2)w)\right) , \tag{4.55}$$

the w integral can now be performed. The result is

$$I = \sum_{n=1,m=0}^{\infty} c_n \frac{(a+i)4^{m-1} a^{2m} \left(a^2+1\right)^{-\frac{1}{4}(4m+n+5)} \Gamma\left(m+\frac{n+1}{4}\right)\Gamma\left(m+\frac{n+1}{2}\right)}{\Gamma(2m+2)\Gamma\left(\frac{7+3n}{4}\right)} \cdot$$
$$\cdot \left(a\left(2m-6mn-2n^2-n+1\right) - i(2m+1)(n+1)\right) \tag{4.56}$$

The sum over m can be expressed in terms of the ordinary hypergeometric function, ${}_2F_1(a_1, a_2; b; z)$:

$$I = \sum_{n=1}^{\infty} c_n \frac{(n+1)\left(a^2+1\right)^{-\frac{n}{4}-\frac{1}{4}} \Gamma\left(\frac{n+1}{4}\right)\Gamma\left(\frac{n+1}{2}\right)}{24(a-i)^2(a+i)\Gamma\left(\frac{3n}{4}+\frac{7}{4}\right)} \cdot$$
$$\cdot \left(a^2(n+1)(-3an+a-i(n+1)) \, {}_2F_1\left(\frac{n+3}{2}, \frac{n+5}{4}; \frac{5}{2}; \frac{a^2}{a^2+1}\right) + \right.$$
$$\left. - 6\left(a^2+1\right)(a(2n-1)+i) \, {}_2F_1\left(\frac{n+1}{4}, \frac{n+1}{2}; \frac{3}{2}; \frac{a^2}{a^2+1}\right) \right) \tag{4.57}$$

The space-time dependence in this expression is implicit in $a = \tau/r$ and with additional r-dependence in the coefficients c_n The result above is the value for both τ and r positive. Using the known symmetries presented above the solution can be extended to all values of τ and r by appropriate absolute value signs. Then changing variables to

$$\begin{aligned} \tau &= R\cos(\Phi) \\ r &= R\sin(\Phi) \end{aligned} \tag{4.58}$$

we have

$$I = \frac{\lambda f\left(R\lambda\sqrt{N_f k_F}, \Phi\right)}{\sqrt{N_f k_F}} \tag{4.59}$$

with the function $f(\tilde{R}, \Phi)$ given by

$$\begin{aligned} f(\tilde{R}, \Phi) =& \sum_{n=1}^{\infty} f_n \tilde{R}^n \\ f_n =& \frac{\pi^{n-2} e^{i\Phi}(-1)^n \Gamma\left(\frac{n+1}{4}\right) |\sin(\Phi)|^{\frac{1+3n}{2}}}{72(3n-1)\Gamma\left(\frac{n}{2}+1\right)\Gamma\left(\frac{1+3n}{4}\right)} \cdot \\ & \cdot \Bigg({}_2F_1\left(\frac{n+3}{2}, \frac{n+5}{4}; \frac{5}{2}; \cos^2(\Phi)\right)(n+1) \cdot \\ & \quad \cdot \cos^2(\Phi)((1-3n)\cos(\Phi) - i(n+1)\sin(\Phi)) \\ & + {}_2F_1\left(\frac{n+1}{4}, \frac{n+1}{2}; \frac{3}{2}; \cos^2(\Phi)\right) 6((1-2n)\cos(\Phi) - i\sin(\Phi)) \Bigg) \end{aligned} \tag{4.60}$$

This exact infinite series expression for the exponent $I(r, \phi)$ gives us the exact fermion two-point function in real (Euclidean) space (time). We have not been able to find a closed form expression for this final series. Note that $f_n \sim 1/n!$ for large n, and the series therefore converges rapidly. Moreover, numerically the hypergeometric functions are readily evaluated to arbitrary precision (e.g. with Mathematica), and therefore the value of f can be robustly evaluated to any required precision.

As a check on this result, we can compare it to the exact result in the quenched $N_f k_F = 0$ limit in [48], where the exact answer was found in a different way. In the limit where $N_f k_F \to 0$ we see that only the first

term of this series gives a contribution and the expression for the exponent collapses to

$$\lim_{N_f \to 0} I(R, \Phi) = \lambda^2 f_1 R = \lambda^2 \frac{e^{2i\Phi}}{12\pi} R \tag{4.61}$$

In Cartesian coordinates this equals

$$\lim_{N_f \to 0} I(\tau, r) = \lambda^2 \frac{(\tau + ir)^2}{12\pi\sqrt{\tau^2 + r^2}} \tag{4.62}$$

This is the exact same expression as found in [48] for $v = 1$.

There is one value of the argument for which f drastically simplifies. For $r = 0$ ($\Phi = 0, \pi$) we have

$$f_n(\Phi = 0) = -\frac{(-2\pi)^{n-2}}{3\Gamma(n+2)} \tag{4.63}$$

and thus

$$f(\tilde{R}, \Phi = 0) = \frac{1}{12\pi^2} + \frac{e^{-2\pi\tilde{R}} - 1}{24\pi^3 \tilde{R}} \tag{4.64}$$

Further numerical analysis shows that the real part of $f(\tau, r)$ is maximal for $r = 0$. Eq. (4.64) can be seen to give a good qualitative description.

The IR limit of the exact fermion two-point function compared to the large-$N_f k_F$ limit

Before turning to the numerical Fourier transform of the exact real space answer, we derive the IR approximation more systematically. The expression obtained above, Eq. (4.60), is not very useful for extracting the IR Greens function or at a large $N_f k_F$ as the expression is organized in an expansion around $R\lambda\sqrt{N_f k_F} = 0$. To study the limit where $R\lambda\sqrt{N_f k_F} \gg 1$ we can go back to Eq. (4.50). With this expression we see that the exponential in the integrand, $e^{-4uz(s)}$ with $z \sim \sqrt{N_f k_F}|sr + \tau| \sim \tilde{r}$, is generically suppressed for large $\tilde{R} = \lambda R\sqrt{N_f k_F}$. The exceptions are when either $sr + \tau$ is small, s is large, or u is small. The first two cases are also unimportant in the $\tilde{R} \gg 1$ limit. In the first case we restrict the s integral to a small range of order $1/\tilde{R}$ around $-\tau/r$; this contribution therefore becomes more and more negligible in the limit $\tilde{R} \gg 1$. In the second case we will have a remaining large denominator in s outside the exponent that

also suppresses the overall integral. Thus for large $\tilde{R}$, the only appreciable contribution of the exponential term to the integral in $I(\tau, r)$ arises when u is small. To use this, we first write the integral as

$$I_{\rm IR} = I_{\rm IR,exp} + I_{\rm IR,-1}, \tag{4.65}$$

with

$$\begin{aligned} I_{\rm IR,exp}(\tau, r) = \lambda \int_{-\infty}^{\infty} {\rm d}s \frac{s-i}{12\pi^3 (s+i)(1+s^2)^{3/4}\sqrt{N_f k_F}} \cdot \\ \cdot \left(\int_0^1 {\rm d}u \frac{{\rm e}^{-4uz(s)}}{u^{4/3}\sqrt{1-u^{4/3}}} - \int_0^{\infty} {\rm d}u \frac{1}{u^{4/3}} \right) \simeq \\ \lambda \int_{-\infty}^{\infty} {\rm d}s \frac{s-i}{12\pi^3 (s+i)(1+s^2)^{3/4}\sqrt{N_f k_F}} \left(\int_0^1 {\rm d}u \frac{{\rm e}^{-4uz(s)}}{u^{4/3}} - \int_0^{\infty} {\rm d}u \frac{1}{u^{4/3}} \right) \end{aligned} \tag{4.66}$$

and

$$\begin{aligned} I_{\rm IR,-1}(\tau, r) = \lambda \int_{-\infty}^{\infty} {\rm d}s \frac{(s-i)}{12\pi^3 (s+i)(1+s^2)^{3/4}\sqrt{N_f k_F}} \cdot \\ \cdot \left(\int_0^{\infty} {\rm d}u \frac{1}{u^{4/3}} + \int_0^1 {\rm d}u \frac{-1}{u^{4/3}\sqrt{1-u^{4/3}}} \right) \end{aligned}$$

We have added and subtracted an extra term to each to ensure convergence of each of the separate terms. Since the important contribution to $I_{\rm IR,exp}$ is from the small u region we can extend its range from (0,1) to $(0, \infty)$. This way, the integrals can then be done

$$\begin{aligned} I_{\rm exp} &= \int_{-\infty}^{\infty} {\rm d}s \frac{-\lambda^{4/3} \left| sr + \tau \right|^{1/3}}{2^{2/3} 3^{3/2} \pi^{5/3} (N_f k_F)^{1/3} (s+i)^2 \Gamma\left(\frac{4}{3}\right)} \\ &= -\frac{\Gamma\left(\frac{2}{3}\right) \lambda^{4/3} \left| r \right|^{1/3}}{2^{2/3} 3^{3/2} \pi^{5/3} (N_f k_F)^{1/3} \left(1 + \frac{i\tau}{r}\right)^{2/3}}, \end{aligned} \tag{4.67}$$

$$\begin{aligned} I_{\rm IR,-1} = \int_{-\infty}^{\infty} {\rm d}s \frac{\lambda (s-i)}{12\pi^3 (s+i)(1+s^2)^{3/4}\sqrt{N_f k_F}} \cdot \\ \cdot \left(\int_0^{\infty} {\rm d}u \left(\frac{1}{u^{4/3}} - \frac{\theta(1-u)}{u^{4/3}\sqrt{1-u^{4/3}}} \right) \right) = \frac{\lambda}{12\pi^2 \sqrt{N_f k_F}} \end{aligned} \tag{4.68}$$

In total we have for large $\tilde{R}$:

$$I = -\frac{\Gamma\left(\frac{2}{3}\right)\lambda^{4/3}\,|r|}{2^{2/3}3^{3/2}\pi^{5/3}(N_f k_F)^{1/3}\left(|r| + i\,\mathrm{sgn}(r)\tau\right)^{2/3}} + \frac{\lambda}{12\pi^2\sqrt{N_f k_F}} + \\ + \mathcal{O}(\lambda^{2/3}(N_f k_F)^{-4/6} r^{-1/3}) \tag{4.69}$$

We see that the leading order term in R is the same as was obtained from the large $N_f k_F$ approximation of the exponent. The first subleading term is just a constant. This is good news because we already have the Fourier transform of this expression. This result is valid for length scales larger than $1/\lambda\sqrt{N_f k_F}$ with a bounded error of the order $R^{-1/3}$. This readily seen. Defining this approximation as G_{IR}, i.e.

$$G_{\mathrm{IR}} = G_0 \exp\left(-\frac{\Gamma\left(\frac{2}{3}\right)\lambda^{4/3}\,|r|}{2^{2/3}3^{3/2}\pi^{5/3}(N_f k_F)^{1/3}\left(|r| + i\,\mathrm{sgn}(r)\tau\right)^{2/3}} + \right. \\ \left. + \frac{\lambda}{12\pi^2\sqrt{N_f k_F}}\right) , \tag{4.70}$$

the error of this approximation follows from:

$$\Delta G_{\mathrm{IR}} = G - G_{\mathrm{IR}} = G_{\mathrm{IR}}\left(\exp\left(\mathcal{O}(\tilde{R}^{-1/3})\right) - 1\right) \tag{4.71}$$

Since the exponential in G_{IR} is bounded we have that $\Delta G_{\mathrm{IR}} = \mathcal{O}(R^{-4/3})$. After Fourier transforming this translates to an error of order $\mathcal{O}(k^{-2/3})$.

4.4.2 The exact fermion two-point function in momentum space: Numerical method

We now turn to the evaluation of the Fourier transformation. As our exact answer is in the form of an infinite sum, this is not feasible analytically. We therefore resort to a straightforward numerical Fourier analysis.

To do so we first numerically determine the real space value of the exact Green's functions. To do so accurately, several observations are relevant

- The coefficients f_n in the infinite sum for $I(\tau, r)$ decay factorially in n so once n is of order $\tilde{R}$, convergence is very rapid.

- The hypergeometric functions for each n are costly to compute with high precision, but with the above choice of polar coordinates the arguments of the hypergeometric functions are independent of R and $N_f k_F$. We therefore numerically evaluate the series over a grid in $\tilde{R}$ and Φ. We can then reuse the hypergeometric function evaluations many times and greatly decrease computing time.

- The real space polar grid will be limited to a finite size. The IR expansion from Eq. (4.70) can be used instead of the exact series for large enough $R\sqrt{N_f k_F}$. To do so, we have to ensure an overlapping regime of validity. It turns out that a rather large value of $r\sqrt{N_f k_F}$ is necessary to obtain numerical agreement between these two expansions, i.e. one needs to evaluate a comparably large number of terms in the expansion. For the results presented in this chapter it has been necessary to compute coefficients up to order 16 000 in $R\sqrt{N_f k_F}$, for many different angles Φ. The function is bounded for large τ and r but each term grows quickly. This means that there are large cancellations between the terms that in the end give us a small value. We therefore need to calculate these coefficients to very high precision in evaluating the polynomial. For these high precision calculations, we have used the Gnu Multiprecision Library.

- On this polar grid we computed the exact answer for $\tilde{R} < \tilde{R}_0 \approx 1000$ and used cubic interpolation for intermediate values. For larger $\tilde{R}$ we use the asymptotic expansion in Eq. (4.70).

- Finally we represent the function values using normal 128 bit complex numbers.

We then use a standard discrete numerical Fourier transform (DFT) to obtain the momentum space two-point function from this numeric prescription for $G(R, \Phi)$. Sampling $G(R, \Phi)$ at a finite number of discrete points, the size of the sampling grid will introduce an IR cut-off at the largest scales we sample and a UV-cut off set by the smallest spacing between points. These errors in the final result can be minimized by using the known asymptotic values analytically. Rather than Fourier transforming $G(\tau, r)$ as a whole, we Fourier transform $G_{\text{diff}}(\tau, r) = G(\tau, r) - G_{\text{IR}}(\tau, r)$ instead. Since both these functions approach the free propagator in the UV, the Fourier transform of its difference will decay faster for large ω and k. This greatly reduces the UV artefacts inherent in a discrete fourier

transform (DFT). These two functions also approach each other for large τ and x. In fact, with the numerical method we use to approximate f described above, they will be identical for $\tilde{R}_0 < \sqrt{N_f k_F(\tau^2 + r^2)}$. This means that we only need to sample the DFT within that area. With a DFT we will always get some of the UV tails of the function giving folding aliasing artefacts. Now our function decays rapidly so one could do a DFT to very high frequencies and discard the high frequency part. This unfortunately takes up a lot of memory so we have gone with a more CPU intensive but memory friendly approach. We instead first perform a convolution with a Gaussian kernel, perform the DFT, keep the lowest 1/3 of the frequencies and then divide by the Fourier transform of the kernel used. This gives us a good numeric value for $G_{\text{diff}}(\omega, k)$. To this we add our analytic expression for $G_{\text{IR}}(\omega, k)$.

4.5 The physics of 2+1 quantum critical metals at large k_F

With the exact analytical real space expression and numerical momentum space expression for the full non-perturbative fermion Green's function, we can now start to discuss the physics of the elementaray quantum critical metal in the limit of large k_F and small N_f. Let us emphasize right away that all our results are in Euclidean space. Although we suspect that a good Lorentzian continuation with a well-defined and consistent spectral function exists of the Euclidean momentum space Green's function, this function is not easily obtainable from our numerical Euclidean result. We leave this for future work. The Euclidean signature Green's function does not visually encode the spectrum directly, but for very low energies/frequencies the Euclidean and the Lorentzian expressions are nearly identical, and we can extract much of the IR physics already from the Euclidean correlation function.

In Figure 4.4 we show density plots of the imaginary part of $G(\omega, k)$ for different values of $N_f k_F$ as well as cross-sections at fixed low ω. For the formal limit $N_f k_F = 0$ we detect three singularities near $\omega = 0$ corresponding with the three Fermi surfaces found in Lorentzian signature in our earlier work [48]. However, for any appreciable value of the dimensionless ratio $N_f k_F/\lambda^2$ one only sees a single singularity. As the plots for $G(\omega, k)$ at low frequency show, its shape approaches that of the strongly Landau-damped RPA result as one increases $N_f k_F/\lambda^2$, though for low

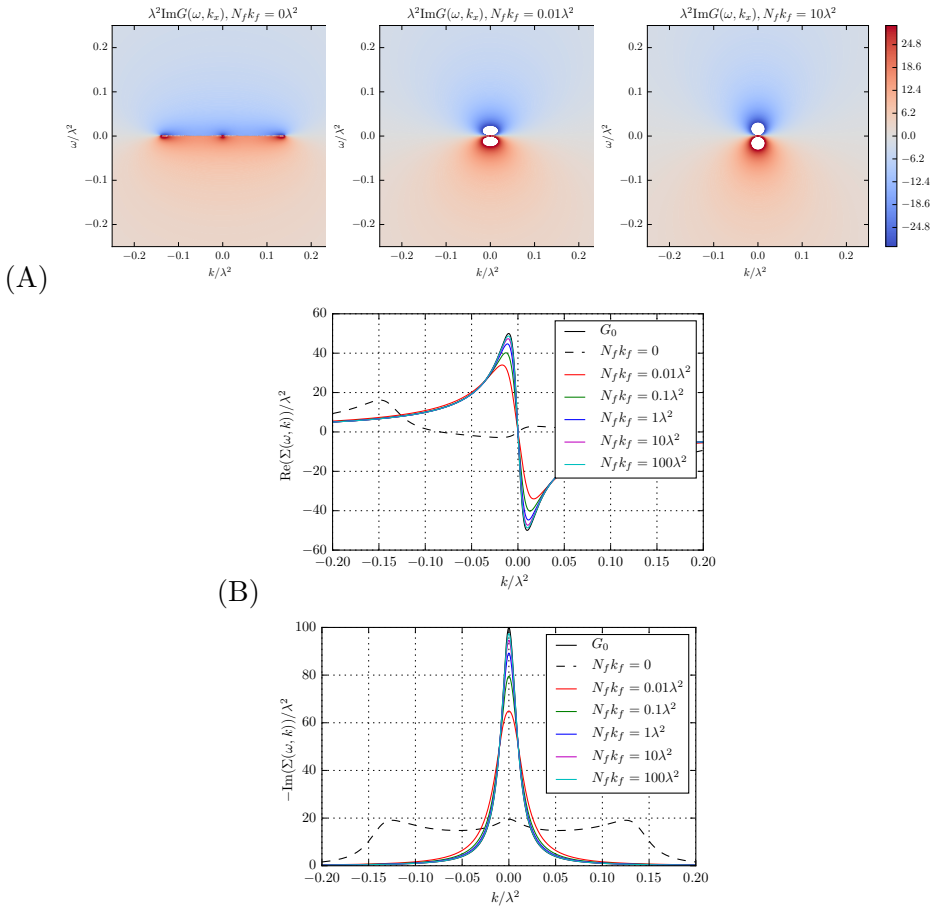

Figure 4.4. (A) Density plots of the imaginary part of the exact (Euclidean) fermion Green's function $G(\omega, k)$ for various values of $N_f k_F$. In the quenched limit $N_f k_F = 0$ the three Fermi surface singularities are visible. For any appreciable finite $N_f k_F$ the Euclidean Green's function behaves as a single Fermi surface non-Fermi liquid. (B) Real and imaginary parts of $G(\omega, k)$ for very small $\omega = 0.01\lambda^2$.

$N_f k_F$ it is still distinguishably different.

This result is in contradistinction to what happens to the bosons. When the bosons are not affected in the IR, i.e. the quenched limit, it is evident that the fermions are greatly affected by the boson: there is a topological Fermi surface transition and the low-energy spectrum behaves as critical excitations [48]. However, once we increase $N_f k_F$, the bosonic

excitations are rapidly dominated in the IR by Landau damping but we now see that this reduces the corrections to the fermions. As $N_f k_F$ is increased, the deep IR fermion two-point function approaches more and more that of the RPA result with self-energy $\Sigma \sim i\omega^{2/3}$.

We can illustrate this more clearly by studying the self-energy of the fermion $\Sigma(\omega, k) = G(\omega, k)^{-1} - G_0(\omega, k)^{-1}$. It is shown that the naive large N_f RPA result (dotted lines) does agree at $\omega = 0, k = 0$ and the leading ω dependence of the imaginary part is captured. The leading k dependence are not captured by RPA. On the other hand, our improved approximation for the low energy regime G_{IR} (dashed lines) captures these higher order terms in the low energy expansion of G very well.

We can calculate the occupation number and check whether it is consistent with the non-Fermi liquid nature of the Green's function. For a Fermi liquid there is a discontinuity in the zero-temperature momentum distribution function $n_k = \int_{-\infty}^{0} \mathrm{d}\omega_R A(\omega_R, k)/2\pi$ with $A(\omega_R, k)$ the spectral function. As the spectral function is the imaginary part of the retarded Green's functions and the latter is analytic in the upper half plane of ω_R we can move this contour to Euclidean ω and use the fact that G approaches G_0 in the UV to calculate the momentum distribution function from our Euclidean results. In detail

$$n_k = -\int_{-\infty}^{0} \mathrm{d}\omega_R \mathrm{Im} \frac{G_R(\omega_R, k)}{\pi} = \mathrm{Im}\left[\int_0^{\Lambda} \mathrm{d}\omega i \frac{G(\omega, k)}{\pi} + \int_C \mathrm{d}z i \frac{G(z, k)}{\pi}\right]; \tag{4.72}$$

the first integral can be done with the numerics developed in the preceding section. The contour C goes from $i\Lambda$ to $-\infty$ and for large enough Λ this is in the UV and can well be approximated by the free propagator. The resulting momentum distribution $n(k)$ is shown in Figure 4.6. Within our numerical resolution, these curves are continuous as opposed to a Fermi liquid. This is of course expected; the continuity reflects the absence of a clear pole in the IR expansions in the preceding subsection. Note also that as $N_f k_F$ is lowered, the finite $N_f k_F$ curves approach the quenched result for $|k| > k^*$ where k^* is the point of the discontinuity of the derivative of the quenched occupation number. At k^* the (derivative) of the quenched momentum distribution number does have a discontinuity (reflecting the branch cut found in [48]).

Our result highlights how various approximations that have been made in the past hang together. In units of the bare coupling λ the $k_F \to \infty$ theory is characterized by two parameters ω/λ^2 and N_f — the latter al-

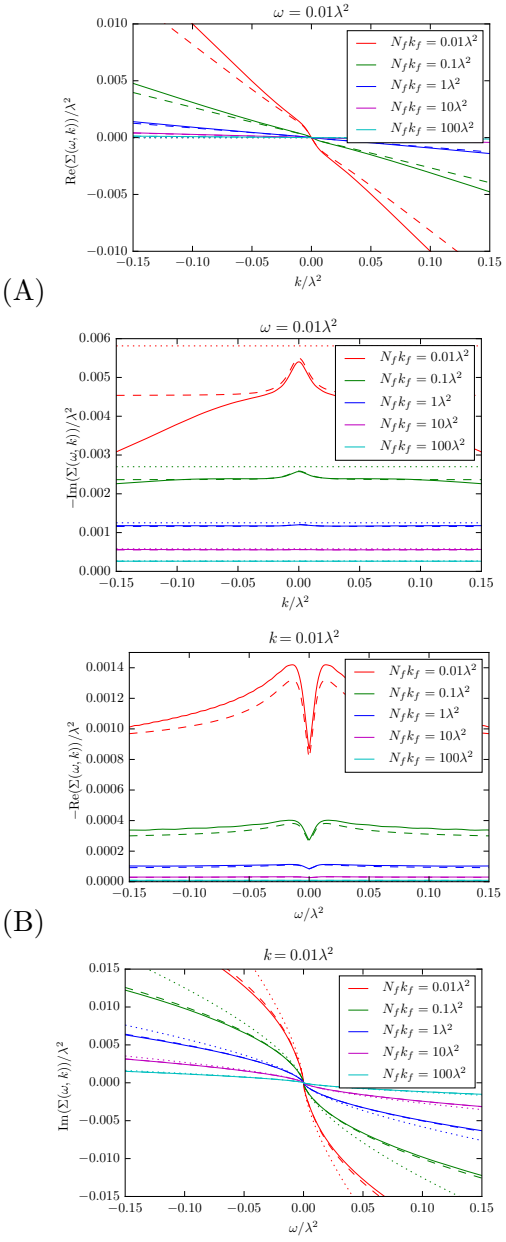

Figure 4.5. Real and imaginary parts of the fermion self-energy for (A) $\omega = 0.01\lambda^2$ and for (B) $k = 0.01\lambda^2$. Dashed lines show the G_{IR}-approximation; dotted lines show the RPA result.

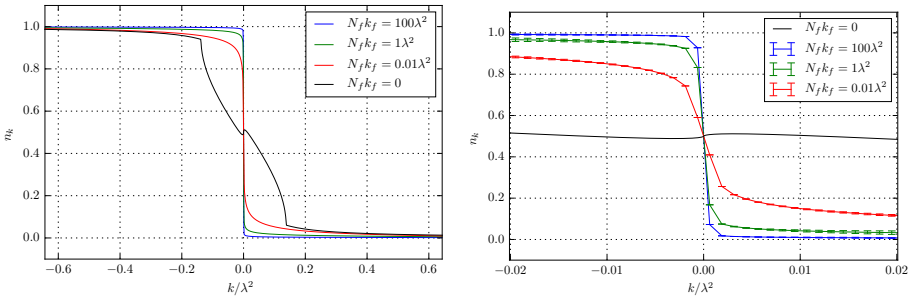

Figure 4.6. Momentum distribution function. The two plots show the same function for different ranges. The error bars of the lower figure show an estimate of the error due to using the free Green's function close to the UV. The error-bars are exaggerated by a factor 100.

ways appears in the combination $N_f k_F/\lambda^2$, and as we explained in section 4.4 we considered this finite even when $k_F/\lambda^2 \to \infty$. For very large ω/λ^2 one can use perturbation theory in λ to understand the theory. This is the perturbation around the UV-fixed point of a free fermion plus a free boson.

For small ω/λ^2 and small $N_f k_F/\lambda^2$ the quenched result we obtained earlier [48] captures the right physics. As the momentum occupation number $n(k)$ indicates, its precise regime of applicability depends discontinuously on the momentum k/λ^2. The discontinuity is surprising, but it can be explained analytically as an order of limits ambiguity. Although it is hard to capture the deep IR region for very small $N_f k_F$ in the full numerics we suspect that in the ω-k plane there is a region where the limit $N_f k_F \to 0$ and $\omega, k \to 0$ do not commute. We show an indication of this in appendix 4.C. Physically this is the scale where Landau damping becomes important.

For small ω/λ^2 the IR approximation presented here captures the physics independently of the value of $N_f k_F/\lambda^2$. For large $N_f k_F/\lambda^2$ the spectrum it predicts closely approximates the known result [38], but improves on it for larger frequencies. We have presented a pictorial overview of how the various approximations are related in Fig.4.7.

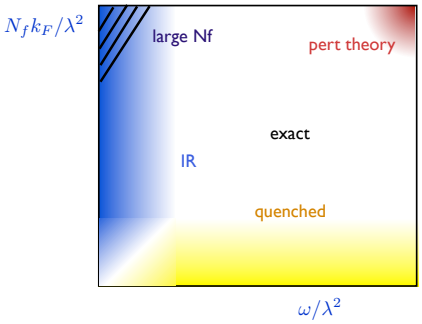

Figure 4.7. A sketch of the regimes of applicability of various approximations to the exact fermion Green's function of the elementary quantum critical metal.

4.6 Conclusion

We have presented a non-perturbative answer for the (Euclidean) fermion and boson two-point functions of the elementary quantum critical metal in the limit of large k_F and small N_f. This non-perturbative answer follows from tracing of the role of the Fermi momentum in the Schwinger-Dyson equations and the fermion number Ward identity. In the limit of large k_F they form a closed set on the boson and fermion two-point functions with the subtle point that the leading one-loop contribution to the boson two-point function (formally divergent as $k_F \to \infty$) needs to be kept. We have presented an analytic expression for the direct IR limit of the Green's functions.

It would be enlightening to have our results in Lorentzian signature (as in the quenced limit); at the technical level this is an obvious next step. At the physics level, an obvious next step is to explore the model without relying on the smallness of N_f and the $k_F \to \infty$ limit. Since this necessarily involves higher-point boson correlations, the role of the self-interactions of the boson needs to be considered. These are also revelant in the IR and may therefore give rise to qualitatively very different physics than found here.

4.A Derivation of the Schwinger-Dyson equations and the Ward Identity

The Schwinger-Dyson equation for the fermion two-point function can be derived from its defining equation in the presence of a background field $\phi(x)$.

$$\left(-\partial_\tau + \frac{\nabla^2}{2m} + \mu + \lambda\phi(x)\right) G[\phi](x,y) = \delta^3(x-y) \tag{4.73}$$

Here $x = \{\tau, \mathbf{x}\}$ etc. In the full theory $\phi(x)$ is a dynamical field and performing the path-integral one obtains

$$\frac{1}{Z_\phi(J)} \int \mathcal{D}\phi \left[(-\partial_\tau + \frac{\nabla^2}{2m} + \mu + \lambda\phi) G[\phi](x,y) - \delta^3(x-y)\right]$$
$$e^{-\int\left[\frac{1}{2}(\partial_\tau\phi)^2 + \frac{1}{2}(\nabla\phi)^2 - J\phi\right]} = \left(-\partial_\tau + \frac{\nabla^2}{2m} + \mu + \lambda\frac{\partial}{\partial J}\right) G_J(x,y) - \delta^3(x-y) = 0 \tag{4.74}$$

with $G_J(x,y)$ the exact fermion two-point function in the presence of a scalar source $J(x)$ and $Z_\phi(J)$ being the partition function of a free scalar. The functional derivative $\dfrac{\partial}{\partial J(x)}$ of the two-point function can be computed using the identity that the two-point function is the inverse of double derivative of the 1PI action $\Gamma[\phi_c, \psi_c, \psi_c^\dagger] = \ln Z(J, J_\psi) - \phi_c J - ...$ with respect to the conjugate fields $\psi_c(y),\ \psi_c^\dagger(x)$

$$\frac{\partial}{\partial J(u)} G_J(x,y) = \frac{\partial}{\partial J(u)} \left(\frac{\partial^2\Gamma}{\partial\psi_c(y)\partial\psi_c^\dagger(x)}\right)^{-1} \tag{4.75}$$

Also for the scalar, the 1PI action depends on the classical Legendre conjugate field $\phi_c(x)$ rather than the source $J(x)$. Using the chain rule, one has

$$\begin{aligned}
\frac{\partial}{\partial J(u)} G_J(x,y) &= \int d^3z \frac{\partial\phi_c(z)}{\partial J(u)} \frac{\partial}{\partial\phi_c(z)} \left(\frac{\partial^2\Gamma}{\partial\psi_c(y)\partial\psi_c^\dagger(x)}\right)^{-1} \\
&= -\int d^3z_1 d^3z_2 d^3z_3 \frac{\partial\phi_c(z_1)}{\partial J(u)} \left(\frac{\partial^2\Gamma}{\partial\psi_c(y)\partial\psi_c^\dagger(z_2)}\right)^{-1} \cdot \\
&\quad \cdot \left(\frac{\partial^3\Gamma}{\partial\phi_c(z_1)\partial\psi_c(z_2)\partial\psi_c^\dagger(z_3)}\right) \left(\frac{\partial^2\Gamma}{\partial\psi_c(z_3)\partial\psi_c^\dagger(x)}\right)^{-1}.
\end{aligned} \tag{4.76}$$

From its definition the conjugate field $\phi_c(z) = \frac{\partial \ln Z}{\partial J(z)}$, we see that $\frac{\partial \phi_c(z)}{\partial J(u)}$ equals the scalar two-point function in the presence of a source J.

$$\frac{\partial \phi_c(z)}{\partial J(u)} = \frac{\partial^2 \ln Z}{\partial J(u) \partial J(z)} = G_{B,J}(z,u) \tag{4.77}$$

Substituting these relations into Eq. (4.76) and the result into (4.74) together with the relation between the double derivative of the 1PI action and the Green's function one obtains

$$\begin{aligned} 0 = -\delta^3(x-y) + \left(-\partial_\tau + \frac{\nabla^2}{2m} + \mu\right) G(x,y) - \\ \lambda G_B(x,z) G(y,z_2) \Lambda(z,z_2,z_3) G(z_3,x) \end{aligned} \tag{4.78}$$

with $\Lambda(z,z_2,z_3) \equiv \frac{\partial^3 \Gamma}{\partial \phi_c(z_1) \partial \psi_c(z_2) \partial \psi_c^\dagger(z_3)}$ equal to the 1PI three-point vertex and we have set the source $J = 0$ at the end. Multiplying by the free fermion Green's function $G_0(x,y)$, the inverse of the free kinetic operator $(-\partial_\tau + \frac{\nabla^2}{2m} + \mu)$ and Fourier transforming we arrive at the equation (4.6) quoted in the main text

$$\begin{aligned} 0 &= -G_0(x,y) + G(x,y) - G_0(x,y) \lambda G_B(x,z) G(y,z_2) \Gamma(z,z_2,z_3) G(z_3,x) \\ &= -G_0(K) + G(K) - \lambda G_0(K) G(K) \int dQ G_B(Q) \Lambda(K, K-Q) G(K-Q) \end{aligned} \tag{4.79}$$

In the main text we use Γ to denote the 1PI three-point vertex, as is conventional. By definition $dQ = \frac{dq_0 d^2 q}{(2\pi)^3}$.

4.B The Fourier transform of the fermion Green's function in the large $N_f k_F$ approximation

We will now show how to perform this Fourier transform. We need to calculate the following integral:

$$\underset{N_f k_F \to \infty}{G_f}(\omega, k) = \int \mathrm{d}\tau \mathrm{d}x \frac{\mathrm{e}^{i(\omega\tau - kx)}}{2\pi(ix - v\tau)} \exp\left(-\frac{|x|}{l_0^{1/3}\left(|x| + iv\,\mathrm{sgn}(x)\tau\right)^{2/3}}\right) \tag{4.80}$$

First we note that integrand is τ-analytic in the region $\{\tau \in \mathbb{C} : \min(0, vx) < \mathrm{Im}(\tau) < \max(0, vx)\}$. Since the integrand necessarily goes to 0 at ∞ we can thus shift the τ contour, $\tau \to \tau + ix/v$. We now have

$$\underset{N_f k_F \to \infty}{G_f}(\omega, k) = -\int \frac{\mathrm{d}\tau \mathrm{d}x}{2\pi v\tau} \exp\left(i\omega\tau - x\left(ik + \omega/v + \frac{\mathrm{sgn}(x)}{l_0^{1/3}\left(iv\,\mathrm{sgn}(x)\tau\right)^{2/3}}\right)\right) \tag{4.81}$$

We have allowed ourselves to choose the order of integration, shift the contour, and then change the order. We see that the x integral now is trivial but only converges for

$$-\frac{v^{1/3}}{2l_0^{1/3}|\tau|^{2/3}} < \mathrm{Re}(\omega) < \frac{v^{1/3}}{2l_0^{1/3}|\tau|^{2/3}} \tag{4.82}$$

This is fine since we know that the final result is ω-analytic in both the right and left open half-planes. As long as we can obtain an answer valid within open subsets of both of these sets we can analytically continue the found solution to the whole half planes. We thus proceed assuming $\mathrm{Re}(\omega)$ is in this range. One can further use symmetries of our expression to relate the left and right ω-half-planes, so to simplify matters, from now on we additionally assume ω to be positive. Let us now consider a negative x, we then see that the τ integral can be closed in the upper half plane and since it is holomorphic there the result will be 0. We can thus limit the x integrals to $\mathbb{R}^+$. We then have

$$\underset{`N_f k_F \to \infty}{G_f}(\omega, k) = \int \mathrm{d}\tau \frac{\mathrm{e}^{i\omega\tau}}{2\pi v\tau} \frac{-1}{a + \frac{1}{l_0^{1/3}(iv\tau)^{2/3}}} \tag{4.83}$$

where $a = ik + \omega/v$. The integrand has a pole at $(i\tau)^{2/3} = -1/(al_0^{1/3}v^{2/3})$. Now break the integral in positive and negative τ and write it as

$$\underset{N_f k_F \to \infty}{G_f}(\omega, k) = \frac{h((-i)^{2/3}u_0^*)^* - h((-i)^{2/3}u_0)}{2\pi v a} \tag{4.84}$$

where

$$\begin{aligned} h(u) &= \int_0^\infty \mathrm{d}\tau \frac{\mathrm{e}^{i\tau}}{\tau + u\tau^{1/3}}, \\ u_0 &= \frac{\omega^{2/3}}{al_0^{1/3}v^{2/3}}. \end{aligned} \tag{4.85}$$

Usng Morera's theorem we can prove that h is holomorphic on $\mathbb{C}/\mathbb{R}^-$. Consider any closed curve C in $\mathbb{C}/\mathbb{R}^-$. We need to show that

$$\int_C \mathrm{d}u h(u) = 0 \tag{4.86}$$

We do this by rotating the contour slightly counter clockwise. For any curve C there is clearly a small $\epsilon > 0$ such that we will still not hit the pole $\tau + u\tau^{1/3} = 0$.

$$\int_C \mathrm{d}u \int_0^{(1+i\epsilon)\infty} \mathrm{d}\tau \frac{\mathrm{e}^{i\tau}}{\tau + u\tau^{1/3}}, \tag{4.87}$$

The piece at ∞ converges without the denominator and thus goes to 0. Since the integral now converges absolutely we can use Fubini's theorem to change the orders of integration

$$\int_0^{(1+i\epsilon)\infty} \mathrm{d}\tau \int_C \mathrm{d}u \frac{\mathrm{e}^{i\tau}}{\tau + u\tau^{1/3}} = 0 \tag{4.88}$$

And since also the integrand is holomorphic on a connected open set containing C the proof is finished.

The function h can for $0 < \arg(u) < 2\pi/3$ be expressed as a Meijer G-function:

$$h(u) = \frac{3}{8\pi^{5/2}} G^{5,3}_{3,5}\left(\begin{matrix} 0, \frac{1}{3}, \frac{2}{3} \\ 0, 0, \frac{1}{3}, \frac{1}{2}, \frac{2}{3} \end{matrix} \middle| -\frac{u^3}{4} \right) \tag{4.89}$$

The G-function has a branch cut at $\mathbb{R}^-$ and because of that we can not easily write $h(u)$ in terms of it since the argument u appears cubed in the argument of the G-function and we know that h is holomorphic on all of $\mathbb{C}/\mathbb{R}-$. We can however express h as an analytic continuation of the G-function past this branch cut, onto the further sheets of its Riemann surface. We will write the G-function as a function with two real arguments, first the absolute value and second the phase of its otherwise complex argument. We will allow the phase to be any real number and when outside the range $[-\pi, \pi]$, we let the function be defined by its analytical continuation to the corresponding sheet. We hereafter omit the

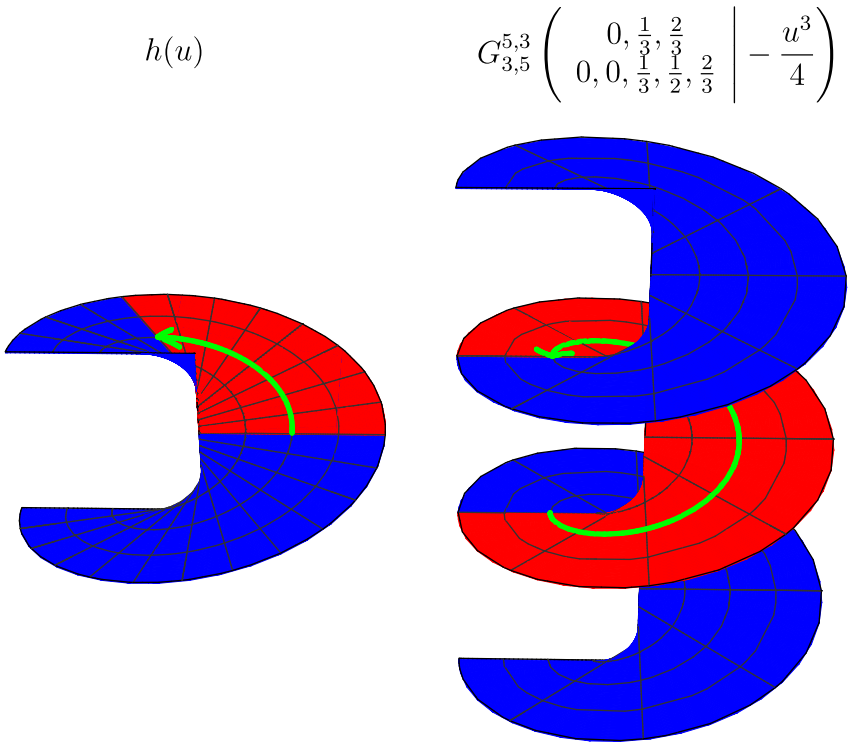

Figure 4.8. The left image shows part of the Riemann surface of the function h and the right image shows part of the Riemann surface of the G-function. The part in red of the left image can be expressed as the G-function evaluated on its first sheet, the red part of the right image. The green arrow shows how points are mapped from one Riemann surface to the other by the mapping $u \mapsto -u^3/4$

constant parameters of the G-function. We then have:

$$\begin{aligned}\underset{N_f k_F \to \infty}{G_f}(\omega, k) &= 3\frac{G_{3,5}^{5,3}\left(\frac{|u_0|^3}{4}, -2\pi - 3\arg(u_0)\right)^* - G_{3,5}^{5,3}\left(\frac{|u_0|^3}{4}, -2\pi + 3\arg(u_0)\right)}{16\pi^{7/2}va} \\ &= 3\frac{G_{3,5}^{5,3}\left(\frac{|u_0|^3}{4}, 3\arg(u_0) + 2\pi\right) - G_{3,5}^{5,3}\left(\frac{|u_0|^3}{4}, 3\arg(u_0) - 2\pi\right)}{16\pi^{7/2}va}\end{aligned} \tag{4.90}$$

In the last step we used the fact that the G-function commutes with complex conjugation. We see that the Green's function is given by a certain monodromy of the G-function. It is given by the difference in its value starting at a point $u_0^3/4$ on the sheet above the standard one and then analytically continuing clockwise around the origin twice to the sheet below the standard one and there return to $u_0^3/4$. Since we only need this difference, we might expect this to be a, in some sense, simpler function as would happen for e.g. monodromies of the logarithm. To see how to simplify this we look at the definition of the G-function. It is defined as an integral along L:

$$G_{p,q}^{m,n}\left(\begin{matrix} a_1, \ldots, a_p \\ b_1, \ldots, b_q \end{matrix} \middle| \, z\right) = \frac{1}{2\pi i}\int_L \frac{\prod_{j=1}^m \Gamma(b_j - s)\prod_{j=1}^n \Gamma(1 - a_j + s)}{\prod_{j=m+1}^q \Gamma(1 - b_j + s)\prod_{j=n+1}^p \Gamma(a_j - s)} z^s \, ds, \tag{4.91}$$

There are a few different options for L and which one to use depends on the arguments. In our case L starts and ends at $+\infty$ and circles all the poles of $\Gamma(b_i - s)$ in the negative direction. Using the residue theorem we can recast the integral to a series. We have double poles at all negative integers and some simple poles in between. The calculation to figure out the residues of all these single and double poles is a bit too technical to present here but in the end the series can be written as

$$G_{3,5}^{5,3}(z) = \sum_{n=0}^{\infty}\left(a_n z^n + b_n z^n \log(z) + c_n z^{n+1/3} + d_n z^{n+1/2} + e_n z^{n+2/3}\right) \tag{4.92}$$

Now we perform the monodromy term by term and a lot of these terms

cancel out.

$$G^{5,3}_{3,5}\Big(|z|,\arg(z)+2\pi\Big)-G^{5,3}_{3,5}\Big(|z|,\arg(z)-2\pi\Big)= \sum_{n=0}^{\infty}\left(4\pi i b_n z^n+i\sqrt{3}c_n z^{n+1/3}-i\sqrt{3}e_n z^{n+2/3}\right) \tag{4.93}$$

The coefficients a_i contain both the harmonic numbers and the polygamma function whereas the other coefficients are just simple products of gamma functions. This simplification now lets us sum this series to a couple of hypergeometric functions. Inserting the expressions for a and u_0 we have

$$\begin{aligned} \underset{N_f k_F\to\infty}{G_f}(\omega,k) &= \frac{1}{i\omega-kv}\cos\left(\frac{\omega}{v l_0^{1/2}(\omega/v+ik)^{3/2}}\right) \\ &+\frac{6\sqrt{3}i\Gamma\left(\frac{1}{3}\right)\omega^{2/3}}{8\pi l_0^{1/3}v^{5/3}(\omega/v+ik)^2}\,{}_1F_2\left(1;\frac{5}{6},\frac{4}{3};-\frac{\omega^2}{4l_0v^2(\omega/v+ik)^3}\right)+ \\ &+\frac{3\sqrt{3}i\Gamma\left(-\frac{1}{3}\right)\omega^{4/3}}{8\pi l_0^{2/3}v^{7/3}(\omega/v+ik)^3}\,{}_1F_2\left(1;\frac{7}{6},\frac{5}{3};-\frac{\omega^2}{4l_0v^2(\omega/v+ik)^3}\right). \end{aligned} \tag{4.94}$$

Note that this expression is ω-holomorphic for ω in the right half plane so our previous assumptions on ω can be relaxed as long as ω is in the right half plane. We note from expression (4.80) that if we change sign on both ω and k and do the changes of variables $\tau\to-\tau$ and $x\to-x$ we end up with the same integral up to an overall minus sign. We can thus get the left half plane result using the relation

$$\underset{N_f k_F\to\infty}{G_f}(-\omega,k)=-\underset{N_f k_F\to\infty}{G_f}(\omega,-k). \tag{4.95}$$

As mentioned in the main text, this expression has been compared with numerics to verify that we have not made any mistakes. See Fig. 4.2. We have also done the two integrals for the Fourier transform in the opposite order, first obtaining a different Meijer G-function then using the G-function convolution theorem to do the second integral. In the end one obtains the same monodromy of the G-function as above.

4.C The discontinuous transition from the quenched to the Landau-damped regime

We show here why the including Landau damping finite N_f physics starting from the quenched $N_f\to 0$ result, is discontinuous in the IR. To do

so we calculate the Green's function by imposing the $N_f \to 0$ limit from the begining. We need to evaluate the Fourier transform integral:

$$G_L(\omega, k) = \int_{-\infty}^{\infty} dx \int_{-L}^{L} d\tau G_0 \exp\left(I_0 + i\omega \cdot \tau - ik \cdot x\right), \tag{4.96}$$

where as before the free propagator is

$$G_0(\tau, x) = -\frac{i}{2\pi} \frac{1}{x + i \cdot \tau} \tag{4.97}$$

and the $N_f \to 0$ limit of the exponent of the real space Green's function:

$$I_0 = \frac{(\tau + i \cdot x)^2}{12\pi\sqrt{\tau^2 + x^2}}. \tag{4.98}$$

Note however that the τ integral is divergent in this limit. Therefore in (4.96) we have introduced a cutoff L in this direction. By looking at the full expansion of I we can see that the natural value of L is of the order $1/\sqrt{N_f}$. For larger values of τ the asymptotic expansion describes I better. We expect that for large enough momenta and frequencies the asymptotic region does not contribute to the Fourier transform and therefore the cutoff can be removed. This naive epxectation however is only partly true. We will shortly see that the region in the $\omega - k$ plane where the cutoff can be removed is more complicated and asymmetric in term of the momenta and frequency.

Let us turn now to the evaluation of (4.96). After making the coordinate change $\tau \to \tau$, $x \to u \cdot \tau$ one of the integral (τ) can be evaluated analytically:

$$G_L(\omega, k) = \int_{-\infty}^{\infty} du \left(I_1(u) + I_2(u) + I_3(u)\right), \tag{4.99}$$

where

$$I_1(u) = \frac{6 \exp\left(ikLu\sqrt{u^2+1} - iL \cdot \omega \cdot \sqrt{u^2+1} - \frac{L(u-i)^2}{12\pi}\right)}{12\pi(u+i)(ku-\omega) + i\sqrt{u^2+1}u + \sqrt{u^2+1}}, \tag{4.100}$$

$$I_2(u) = \frac{6i \exp\left(-ikLu\sqrt{u^2+1} + iL \cdot \omega \cdot \sqrt{u^2+1} - \frac{L(u-i)^2}{12\pi}\right)}{12i\pi k(u+i)u + \sqrt{u^2+1}u - i\sqrt{u^2+1} + 12\pi(1-iu)\omega}, \tag{4.101}$$

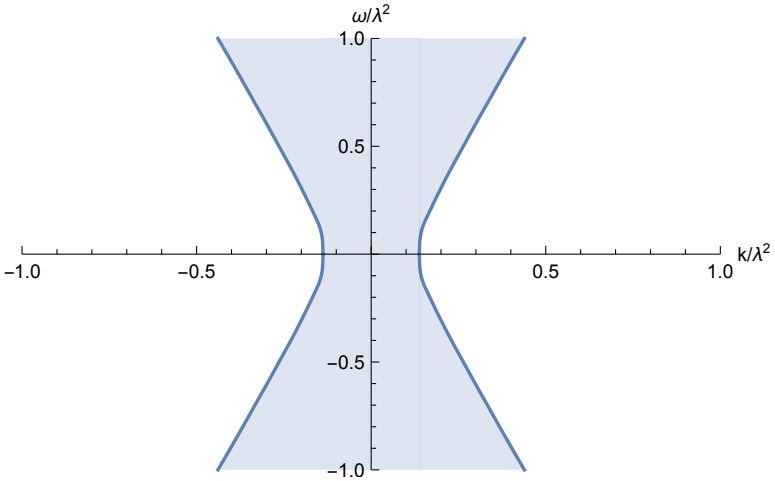

Figure 4.9. The region of convergence. In the shaded area the $L \to \infty$ ($N_f \to 0$) limit is not convergent while outside this area $\lim_{L\to\infty} G_L = G_{quenched}$.

$$I_3(u) = -\frac{144\pi(ku-\omega)}{D(u)}, \tag{4.102}$$

with

$$\begin{aligned} D(u) = u\left(-3 + u\left(144\pi^2 k^2(u+i) + u - 3i\right)\right) \\ -288\pi^2 ku(u+i)\omega + 144\pi^2(u+i)\omega^2 + i. \end{aligned} \tag{4.103}$$

By numerically performing the single integral u we can obtain $G_{N_f\to 0}$. Since it is easier than evaluating the Fourier transform of the true real-space version of the Green's function it is worth to understand how the $L \to \infty$ (which is equivalent to $N_f \to 0$) works. The result is depicted on Fig. 4.9. In the shaded region (which corresponds to small k) the limit is not well defined while outside of this region the limit is equal to the quenched result. The numerics shows that for zero frequency, the edge of this region is at k^*, where the Green's function is singular.

We can qualitatively determine the line separating the convergent and divergent region. For this we assume that when L is large one can expand the exponent in u

$$I_1(u) \sim \exp\left[u^2\left(-\frac{1}{12\pi} - \frac{1}{2}i\omega\right)L + \frac{iu(6\pi k+1)}{6\pi}L - iL\omega + \frac{L}{12\pi} + \mathcal{O}\left(Lu^3\right)\right]. \tag{4.104}$$

We see that because of the term $-L \cdot u^2/(12\pi)$, the integrand is non-zero only in a narrow region around $u = 0$. For the same reason we approximate the denominator of (4.100) by replace u by zero there. With these simplifications we arrive to a gaussian integral which can be evaluated analytically:

$$\int_{-\infty}^{\infty} I_1(u)du \approx \frac{12i\sqrt{3}\pi \exp\left(\frac{iL\left(6\pi k^2+2k+\omega(-12\pi\omega+i)\right)}{12\pi\omega-2i}\right)}{(12\pi\omega+i)\sqrt{L(1+6i\pi\omega)}}. \tag{4.105}$$

The real part of (4.105) is

$$L\frac{3\left(\omega^2-k^2\right)\pi-k}{36\pi^2\omega^2+1}. \tag{4.106}$$

It is clear that if this value is positive (i.e. $3\left(\omega^2-k^2\right)\pi-k>0$) than the $L\to\infty$ limit is divergent. Looking at the numerical result in Fig. 4.9 we indeed see that the boundary of the shaded region is indeed a hyperbola. Note, however, that the exact location of this hyperbola obtained from expanding the exponent is slightly off.

It is interesting to note that if we are in the divergent region G_L is not convergent for large L but for some intermediate values it can still get close to the quenched result $G_{quenched}$. To quantify this let us introduce a relative "error" function

$$error(L) = \left|\frac{G_L - G_{quenched}}{G_{quenched}}\right|. \tag{4.107}$$

In Fig. 4.10 we shows the behavior of this function for various points in the $\omega - k$ plane. For a point which is outside the shaded region the error approaches zero when L is large. For $\omega = 1$, $k = 0$ which is inside the divergent region the error is oscillating but there is an interval of L where the amplitude of this oscillation has a minimum. If the frequency is small ($\omega = 0.1$), this amplitude is larger and there is minimum in that.

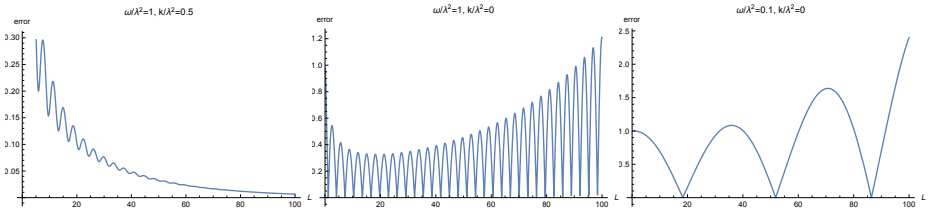

Figure 4.10. The relative difference between G_L and the quenched result as a function of L for different frequencies and momenta. Left: for a point in the (ω, k) plane which is outside of the shaded region of Fig. 4.9 the "error" goes to zero for large L. Middle: inside the shaded region the error is oscillating with diverging amplitude as L goes for large values. However, for larger values of ω there is an intermediate range of L, where the relative error is smaller than 0.3. Therefore the quenched approximation is qualitatively correct. Right: for small ω the amplitude of the oscillation is become large.

Bibliography

[1] S. Sur and S. S. Lee, "Chiral non-Fermi liquids," Phys. Rev. B **90**, no. 4, 045121 (2014) [arXiv:1310.7543 [cond-mat.str-el]].

[2] J. Polchinski, "Effective field theory and the Fermi surface," In *Boulder 1992, Proceedings, Recent directions in particle theory* 235-274, and Calif. Univ. Santa Barbara - NSF-ITP-92-132 (92,rec.Nov.) 39 p. (220633) Texas Univ. Austin - UTTG-92-20 (92,rec.Nov.) 39 p [hep-th/9210046].

[3] R. Shankar, "Renormalization group approach to interacting fermions," Rev. Mod. Phys. **66**, 129 (1994).

[4] J. Hertz, "'Quantum critical phenomena',Phys. Rev. B4, 1165 (1976).

[5] A. J. Millis, "Effect of a nonzero temperature on quantum critical points in itinerant fermion systems",Phys. Rev. **B48**, 7183 (1993).

[6] H. v. Löhneysen, A. Rosch, M. Vojta, P. Wölfle, "Fermi-liquid instabilities at magnetic quantum phase transitions," Rev. Mod. Phys. **79**, 1015 (2007).

[7] L. D. Landau, "The theory of a Fermi liquid," Sov. Phys. Jetp-Ussr **3(6)**, 920-925 (1957)

[8] C. M. Varma, P. B. Littlewood, S. Schmitt-Rink, E. Abrahams and A. E. Ruckenstein, "Phenomenology of the normal state of Cu-O high-temperature superconductors," Phys. Rev. Lett. **63** (1989) 1996

[9] Y. Barlas and K. Yang, "Non-Fermi-liquid behavior in neutral bilayer graphene," Phys. Rev. B **80** (2009) 161408(R); arXiv:0908.1238 [cond-mat.mes-hall]

[10] F. Guinea and M. I. Katsnelson, "Many-Body Renormalization of the Minimal Conductivity in Graphene," Phys. Rev. Lett. **112** (2014) 116604; arXiv:1307.6221 [cond-mat.mes-hall]

[11] D. van der Marel, H. J. A. Molegraaf, J. Zaanen, Z. Nussinov, F. Carbone1, A. Damascelli, H. Eisaki, M. Greven, P. H. Kes, M. Li "Quantum critical behaviour in a high-Tc superconductor," Nature 425, 271-274 (2003); arXiv:cond-mat/0309172

[12] P. Gegenwart, Q. Si, F. Steglich, "Quantum criticality in heavy-fermion metals," Nature Physics 4, 186 - 197 (2008); arXiv:0712.2045 [cond-mat.str-el]

[13] T. Senthil, "Theory of a continuous Mott transition in two dimensions," Phys. Rev. B **78** (2008) 045109; arXiv:0804.1555 [cond-mat.str-el]

[14] T. Misawa and M. Imada, "Quantum criticality around metal–insulator transitions of strongly correlated electron systems," Phys. Rev. B **75** (2007) 115121; arXiv:cond-mat/0612632

[15] J. A. Hertz, "Quantum critical phenomena," Phys. Rev. B **14** (1976) 1165

[16] S. Sachdev, "Quantum phase transitions," Second edition, Cambridge University Press, 2011.

[17] J. Rech, C. Pepin, A. V. Chubukov, "Quantum critical behavior in itinerant electron systems: Eliashberg theory and instability of a ferromagnetic quantum critical point," Phys. Rev. B, f74(19) (2006) 195126; arXiv:cond-mat/0605306

[18] S. Chakravarty, B. I. Halperin and D. R. Nelson, "Two-dimensional quantum Heisenberg antiferromagnet at low temperatures," Phys. Rev. B **39** (1989) 2344

[19] Q. Si, J. L. Smith, K. Ingersent, "Quantum critical behavior in Kondo systems," Int. J. Mod. Phys. B **13** (1999) 2331; arXiv:cond-mat/9905006

[20] M. A. Metlitski and S. Sachdev, "Quantum phase transitions of metals in two spatial dimensions: I. Ising-nematic order," Phys. Rev. B **82** (2010) 075127 arXiv:1001.1153 [cond-mat.str-el]

[21] M. A. Metlitski and S. Sachdev, "Quantum phase transitions of metals in two spatial dimensions: II. Spin density wave order," Phys. Rev. B **82** (2010) 075128 arXiv:1005.1288 [cond-mat.str-el]

[22] T. Holder and W. Metzner, "Anomalous dynamical scaling from nematic and U(1)-gauge field fluctuations in two dimensional metals," Phys. Rev. B **92** (2015) 4, 041112 arXiv:1503.05089 [cond-mat.str-el]

[23] T. Holder and W. Metzner, "Fermion loops and improved power-counting in two-dimensional critical metals with singular forward scattering," arXiv:1509.07783 [cond-mat.str-el]

[24] S. S. Lee, "Low-energy effective theory of Fermi surface coupled with U(1) gauge field in 2+1 dimensions," Phys. Rev. B **80** (2009) 165102; arXiv:0905.4532 [cond-mat.str-el]

[25] D. F. Mross, J. McGreevy, H. Liu and T. Senthil, "A controlled expansion for certain non-Fermi liquid metals," Phys. Rev. B **82** (2010) 045121; arXiv:1003.0894 [cond-mat.str-el]

[26] A. L. Fitzpatrick, S. Kachru, J. Kaplan and S. Raghu, "Non-Fermi liquid fixed point in a Wilsonian theory of quantum critical metals," Phys. Rev. B **88** (2013) 125116 arXiv:1307.0004 [cond-mat.str-el]

[27] A. L. Fitzpatrick, S. Kachru, J. Kaplan and S. Raghu, "Non-Fermi-liquid behavior of large-N_B quantum critical metals," Phys. Rev. B **89** (2014) 16, 165114 arXiv:1312.3321 [cond-mat.str-el]

[28] R. Mahajan, D. M. Ramirez, S. Kachru and S. Raghu, "Quantum critical metals in $d = 3 + 1$ dimensions," Phys. Rev. B **88** (2013) 11, 115116 arXiv:1303.1587 [cond-mat.str-el]

[29] G. Torroba and H. Wang, "Quantum critical metals in $4 - \epsilon$ dimensions," Phys. Rev. B **90** (2014) 16, 165144 arXiv:1406.3029 [cond-mat.str-el]

[30] J. P. Blaizot and E. Iancu, "The Bloch-Nordsieck propagator at finite temperature," Phys. Rev. D **56** (1997) 7877 arXiv:hep-ph/9706397

[31] M. F. L. Golterman, "Chiral perturbation theory and the quenched approximation of QCD," Acta Phys. Polon. B **25**, 1731 (1994) arXiv:hep-lat/9411005

[32] A. Jakovac and P. Mati, "Resummations in the Bloch-Nordsieck model," Phys. Rev. D **85** (2012) 085006 arXiv:1112.3476 [hep-ph]

[33] A. Kernemann and N. G. Stefanis, "Exact Solutions for Fermionic Green's Functions in the Bloch-nordsieck Approximation of QED," Phys. Rev. D **40** (1989) 2103

[34] A. Jakovác and P. Mati, "Spectral function of the Bloch-Nordsieck model at finite temperature," Phys. Rev. D **87** (2013) 12, 125007 arXiv:1301.1803 [hep-th]

[35] A. I. Karanikas, C. N. Ktorides and N. G. Stefanis, "On the infrared structure of the one fermion Green's function in QED," Phys. Lett. B **289** (1992) 176

[36] D. V. Khveshchenko and P. C. E. Stamp, "Low-energy properties of two-dimensional fermions with long-range current-current interactions", Phys. Rev. Lett. **71** (1993) 2118

[37] L. B. Ioffe, D. Lidsky, B. L. Altshuler, "Effective lowering of the dimensionality in strongly correlated two dimensional electron gas", arXiv:cond-mat/9403023.

[38] B. L. Altshuler, L. B. Ioffe, A. J. Millis, "On the low energy properies of fermions with singular interactions", Phys. Rev. **B50**, 14048. arXiv:cond-mat/9406024.

[39] A. Allais and S. Sachdev, "Spectral function of a localized fermion coupled to the Wilson-Fisher conformal field theory," Phys. Rev. B **90** (2014) 3, 035131 arXiv:1406.3022 [cond-mat.str-el]

[40] J. Quintanilla and A. J. Schofield, "Pomeranchuk and topological Fermi surface instabilities from central interactions," Phys. Rev. B **74** (2006) 115126; arXiv:cond-mat/0601103 [cond-mat.str-el]

[41] S. A. Maier and P. Strack, "Universality in antiferromagnetic strange metals," arXiv:1510.01331 [cond-mat.str-el]

[42] A. H. Castro Neto and E. Fradkin, "Bosonization of Fermi liquids," Phys. Rev. B **49** (1994) 10877

[43] A. L. Fitzpatrick, S. Kachru, J. Kaplan, S. Raghu, G. Torroba and H. Wang, "Enhanced Pairing of Quantum Critical Metals Near d=3+1," Phys. Rev. B **92** (2015) 4, 045118 arXiv:1410.6814 [cond-mat.str-el]

[44] M. A. Metlitski, D. F. Mross, S. Sachdev and T. Senthil, "Cooper pairing in non-Fermi liquids," Phys. Rev. B **91** (2015) 11, 115111 arXiv:1403.3694 [cond-mat.str-el]

[45] J. Fröhlich and R. Götschmann, "Bosonization of Fermi liquids," Phys. Rev. B **55** (1997) 6788

[46] S. Raghu, G. Torroba and H. Wang, "Metallic quantum critical points with finite BCS couplings," arXiv:1507.06652 [cond-mat.str-el]

[47] C. Drukier, L. Bartosch, A. Isidori and P. Kopietz, "Functional renormalization group approach to the Ising-nematic quantum critical point of two-dimensional metals," Phys. Rev. B **85** (2012) 245120 arXiv:1203.2645 [cond-mat.str-el]

[48] B. Meszena, P. Säterskog, A. Bagrov and K. Schalm, "Non-perturbative emergence of non-Fermi liquid behaviour in $d = 2$ quantum critical metals," Phys. Rev. B **94**, 115134, [arXiv:1602.05360 [cond-mat.str-el]].

[49] W. Metzner, C. Castellani, C. Di Castro, "Fermi Systems with Strong Forward Scattering", Adv. in Physics **47** 317 (1998). [arXiv:cond-mat/9701012]

[50] T. Holder, W. Metzner "Fermion loops and improved power-counting in two-dimensional critical metals with singular forward scattering" Phys. Rev. **B92**, 245128 (2015). [arXiv:1509.07783 [cond-mat.str-el]]

[51] P. A. Lee, "'Gauge field, Aharonov-Bohm flux, and high-T_c superconductivity', Phys. Rev. Lett. **63**, 680 (1989).

[52] V. Oganesyan, S. Kivelson, E. Fradkin, "Quantum theory of a nematic Fermi fluid", Phys. Rev. B **64**, 195109 (2001).

[53] W. Metzner, D. Rohe, S. Andergassen, "Soft Fermi surfaces and breakdown of Fermi-liquid behavior", Phys. Rev. Lett. **91**, 066402 (2003).

[54] A. Neumayr and W. U. Metzner, "Fermion loops, loop cancellation and density correlations in two-dimensional Fermi systems,' Phys. Rev. B **58** (1998) 15449 [cond-mat/9805207]

[55] Y. B. Kim, A. Furusaki, X. G. Wen and P. Lee, "'Gauge-invariant response function of fermions coupled to a gauge field', Phys. Rev. B **50** (1994) 17917, [arXiv:cond-mat/9405083]

[56] A. L. Fitzpatrick, G. Torroba and H. Wang, "Aspects of Renormalization in Finite Density Field Theory," Phys. Rev. B **91**, 195135 (2015) [arXiv:1410.6811 [cond-mat.str-el]].